AD-A031 331 OHIO STATE UNIV COLUMBUS DEPT OF GEODETIC SCIENCE F/G 8/5
GEODETIC ACCURACIES OBTAINABLE FROM MEASUREMENTS OF FIRST AND S--ETC(U
AUG 76 K SCHWARZ F19628-76-C-0010
UNCLASSIFIED DGS-242 AFGL-TR-76-0189 NL

1 OF 1
ADA031331

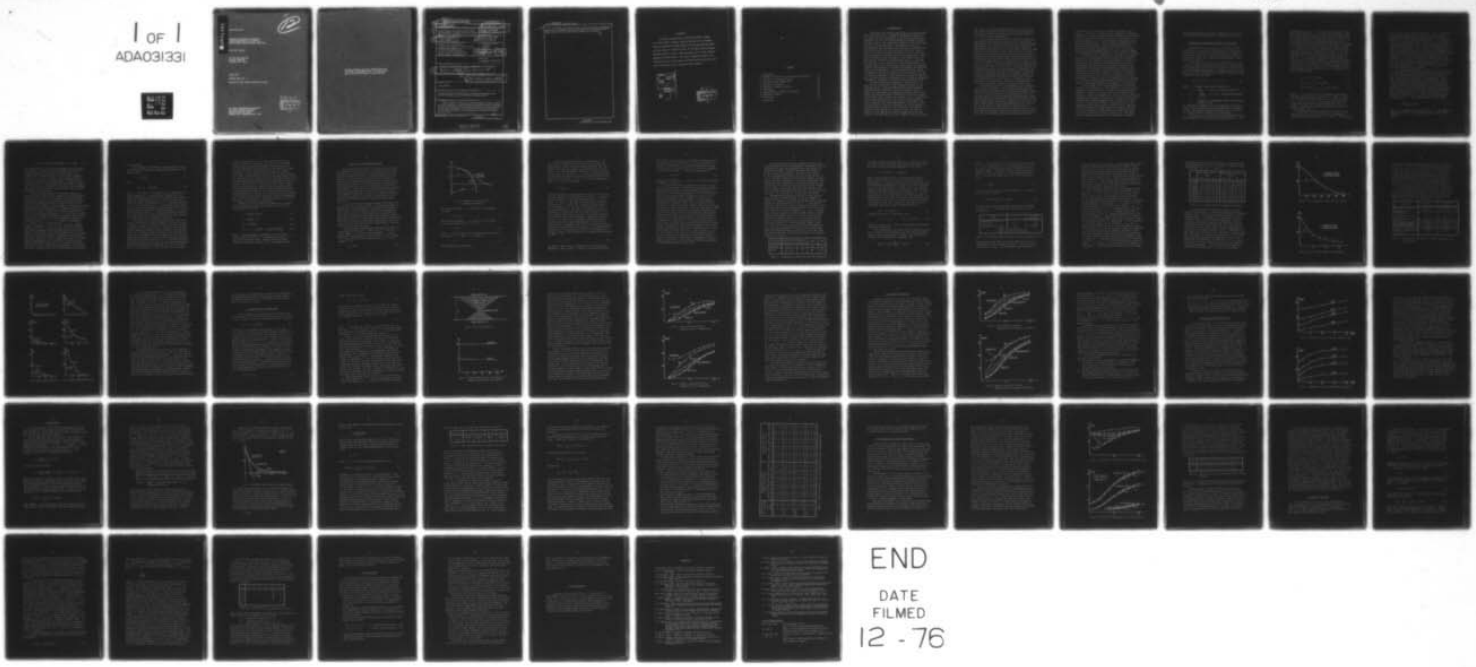

END

DATE
FILMED
12 - 76

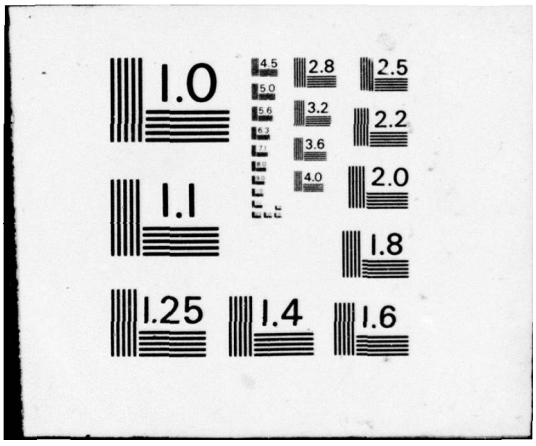
1.0
1.1
1.25
1.4
1.6
1.8
2.0
2.2
2.5
2.8
3.2
3.6
4.0
4.5
5.0
5.6

FG

12

AFGL-TR-76-0189

GEODETIC ACCURACIES OBTAINABLE FROM MEASUREMENTS OF FIRST AND SECOND ORDER GRAVITATIONAL GRADIENTS

Klaus-Peter Schwarz

The Ohio State University
Research Foundation
Columbus, Ohio 43212

August 1976

Scientific Report No. 4

AIR FORCE GEOPHYSICS LABORATORY
AIR FORCE SYSTEMS COMMAND
UNITED STATES AIR FORCE
HANSCOM AFB, MASSACHUSETTS 01731

Unclassified

SECURITY CLASSIFICATION OF THIS PAGE (When Data Entered)

REPORT DOCUMENTATION PAGE

READ INSTRUCTIONS BEFORE COMPLETING FORM

1. REPORT NUMBER: AFGL-TR-76-0189	2. GOVT ACCESSION NO.
3. RECIPIENT'S CATALOG NUMBER	
4. TITLE (and Subtitle): GEODETIC ACCURACIES OBTAINABLE FROM MEASUREMENTS OF FIRST AND SECOND ORDER GRAVITATIONAL GRADIENTS,	5. TYPE OF REPORT & PERIOD COVERED: Scientific. Interim. Scientific Report No. 4
	6. PERFORMING ORG. REPORT NUMBER: Report No. 242
7. AUTHOR(s): Klaus-Peter Schwarz	8. CONTRACT OR GRANT NUMBER(s): F19628-76-C-0010
9. PERFORMING ORGANIZATION NAME AND ADDRESS: Department of Geodetic Science, The Ohio State University - 1958 Neil Avenue, Columbus, Ohio 43210	10. PROGRAM ELEMENT, PROJECT, TASK AREA & WORK UNIT NUMBERS: P76000302, 62101F
11. CONTROLLING OFFICE NAME AND ADDRESS: Air Force Geophysics Laboratory, Hanscom AFB, Massachusetts 01731, Contract Monitor: Bela Szabo/LW	12. REPORT DATE: August 1976
	13. NUMBER OF PAGES: 59 pages
14. MONITORING AGENCY NAME & ADDRESS (if different from Controlling Office)	15. SECURITY CLASS. (of this report): Unclassified
	15a. DECLASSIFICATION/DOWNGRADING SCHEDULE

16. DISTRIBUTION STATEMENT (of this Report)

Approved for public release; distribution unlimited

DGS-242, Scientific-4

17. DISTRIBUTION STATEMENT (of the abstract entered in Block 20, if different from Report)

OSURF-4214A1

18. SUPPLEMENTARY NOTES

TECH, OTHER

19. KEY WORDS (Continue on reverse side if necessary and identify by block number)

airborne gradiometry, satellite altimetry, combination of heterogeneous data, downward continuation, mean value estimation, stability problems.

20. ABSTRACT (Continue on reverse side if necessary and identify by block number)

The accuracy of an airborne accelerometer-gradiometer system is studied for geodetic applications. A detailed analysis of interpolation, downward continuation and mean value determination is given using the method of least-squares collocation. The influence of measuring errors is considered and the effects are contribution of accurate satellite altimetry to a combined accelerometer-gradiometer system is taken into account.

(con't)

DD FORM 1 JAN 73 1473 EDITION OF 1 NOV 65 IS OBSOLETE

Unclassified

SECURITY CLASSIFICATION OF THIS PAGE (When Data Entered)

400254

cont.

The results of this study show that a system of this kind can significantly contribute to our knowledge of the anomalous gravity field if second-order gravitational gradients can be measured with an accuracy of a few Eotvos.

FOREWORD

This report was prepared by Dr. Klaus-Peter Schwarz, assistant to Dr. Helmut Moritz, Professor, Technical University at Graz and Adjunct Professor, Department of Geodetic Science of The Ohio State University, under Air Force Contract No. F19628-76-C-0010, The Ohio State University Research Foundation Project No. 4214A1, Project Supervisor, Urho A. Uotila, Professor, Department of Geodetic Science. The contract covering this research is administered by the Air Force Geophysics Laboratory (AFGL), Hanscom Air Force Base, Massachusetts, with Mr. Bela Szabo, Contract Monitor.

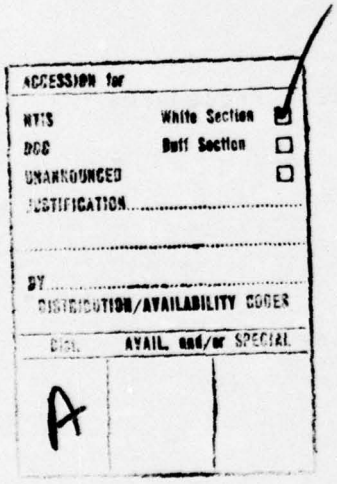

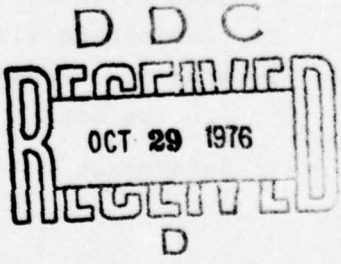

CONTENTS

1. Introduction

Experiments with airborne gravimeters have been performed over the last 15 years. Although the equipment designed for this objective has a high degree of sophistication, the results obtained so far are not accurate enough for geodetic purposes. The reason lies in the complicated structure of the force field acting on a moving gravimeter. Gravimeters are basically accelerometers and they measure the resultant of gravitational and inertial forces. If they are used as stationary instruments, as in most terrestrial applications, the only inertial force acting on the gravimeter is the centrifugal force. Therefore, the output of the instrument is the combined effect of gravitational attraction and centrifugal force, i.e. gravity. The situation is more complicated in a moving gravimeter. The Coriolis force has to be taken into account and, more important, irregular accelerations of the base will strongly influence the result of the measurements. Such undesirable inertial forces are especially strong in a moving aircraft and there is no way to rigorously separate the gravitational part from the inertial part by using gravimeter measurements only. Therefore, additional information is necessary to extract the gravitational effect.

Two methods have been proposed to reach this goal. In the first one information on the frequency behaviour of the different forces is used to separate gravity and disturbing accelerations by statistical filtering techniques. Meissl (1970) has investigated this approach using the theory of stochastic processes and certain assumptions on the power spectra of the force fields involved. He concludes that it is most difficult to separate gravitation and inertia in the medium frequency range with half wavelength between 30 and 150 km. This is only possible if detailed information on the two spectra is available which usually will not be the case. The high frequencies can be blocked by a low pass filter, the low frequencies can be improved by regularly updating altitude and position. The remaining errors will, however, be of a size which

will not allow a useful geodetic application of the filtered data. These findings from a probabilistic error analysis were confirmed by results obtained by Szabo and Anthony (1971) in an analysis of actual measurements.

In the second method structural differences between the gravitational and inertial fields are used to separate the two effects. These differences show up in the second and higher order gradients of the force fields. Therefore, additional measurements are necessary in this case. Moritz (1967) has shown that for an aircraft with inertial stabilization the second derivatives of the force field do not contain inertial disturbances, so that purely gravitational second-order gradients can be measured. They are used to obtain the gravitational force vector by integrating along the flight path. It should be noted that, in contrast to the first method, a rigorous separation of gravitation and inertia is possible in this case, and that from a theoretical point of view this approach is preferable. The practical difficulties originate in the design of instruments accurate enough to make an application feasible. Advances in instrument development have been rapid during the last years and a gradiometer with an accuracy of a few Eotvos may be available in the near future. Therefore, the capabilities of an airborne gradiometer system are studied in this report.

The accuracy study will be performed using the method of least-squares collocation. There are three reasons why this approach seems to be especially suited for the problem at hand. First, it allows the combination of heterogeneous data in a consistent way. This is very important because geoidal heights, gravity anomalies, and different second-order gradients will be used as measurements. They must be evaluated in such a way that their common origin from the same anomalous gravity field is part of the system. In least-squares collocation this is achieved by describing the statistical structure of the field by a covariance function. Second, mean gravity values at ground level must be estimated using point values on a profile in

flying altitude and additional information on ground. This involves interpolation between profiles, downward continuation, combination of different quantities, and estimation of mean values. All these steps can be united in a single step procedure in the collocation method. This is impossible when using the corresponding integral formulas. Third, different assumptions on the structure of the gravity field and on the accuracy of the measurements must be investigated. Again this is very simple with the collocation method because it only involves a change of the fundamental covariance function or of the error variances.

Basically, this is a deterministic approach. Its results are valid if the assumptions on the structure of the gravity field and on the accuracy of the measurements are not too far from reality. The covariance functions have been varied in a rather wide range so that they will hopefully satisfy these requirements. Therefore,no investigations are made as to the influence of an incorrect covariance function. If necessary, results published in Moritz (1976) can be used as a guideline for the present case. The influence of measuring errors will be analysed in a special section. A probabilistic error analysis has not been attempted because adequate information on the error processes affecting gradiometer measurements is not available.

A short survey of the following sections will conclude this part. An introduction to the mathematical structure of the problem is given in section 2. Section 3 discusses the determination of a spatial covariance function from empirical data. Since this section is fundamental for the rest of the report, the arguments are presented in some detail. The mechanism of spatial interpolation using heterogeneous data is studied in sections 4 and 5. In section 6 the effect of measuring errors is discussed and results are applied in sections 7 and 8. Questions related to the design of experiments are treated in section 7 as e.g. the spacing of flight profiles to obtain mean values of certain accuracies for blocks of given sizes. The contribution of highly accurate satellite altimetry to a combined

accelerometer-gradiometer system is considered in section 8. Finally, some numerical problems are summarized in section 9.

2. Mathematical Background and Numerical Procedure.

The objective of this section is to present the main formulas and to discuss their implications. This may serve as a simplified introduction into the mathematical structure of the problem. No derivations are given. They can be found in Moritz (1971, 1975). For a deeper understanding Moritz (1967) should be consulted.

It has been indicated in the introduction why it is not possible to separate gravitation and inertia by using accelerometer measurements only. Let us now consider in which way the use of gradiometer measurements will change the situation. This may best be seen from the system of ordinary differential equations given in Moritz (1975)

$$T_{ij}^{(-1)}\ddot{T}_j + \dot{T}_{ij}^{(-1)}\dot{T}_j - T_i + f_i = 0 \qquad 2.1$$

where T ... anomalous gravitational potential;

T_i ... $= \frac{\partial T}{\partial x_i}$ $\quad i = 1,2,3$ first-order gradients of T;

T_{ij} ... $= \frac{\partial^2 T}{\partial x_i \partial x_j}$ $\quad i,j = 1,2,3$ second-order gradients of T;

f_i ... component of accelerometer output (gravitational + inertial force).

All quantities in equation (2.1) are regarded as functions of time. The dots therefore denote differentiation with respect to time. The summation convention has been used, i.e. an index occuring twice in a product implies summation.

Equation (2.1) is a system of linear second-order differential equations for the gravity disturbance vector T_j. If

the quantities f_i and T_{ij} are given by measurement and the matrix with elements T_{ij} is assumed to be invertible, equation (2.1) may be solved by the usual numerical methods. Thus, it is indeed possible to separate gravitation and inertia, obtaining as a result the purely gravitational quantities T_i, i.e. the deflections of the vertical and the gravity disturbance which usually is not very different from the gravity anomaly.

The practical solution of equation (2.1) may pose some problems. First of all, we need initial values T_i^o at time t_o which may be difficult to get. Second, besides the measured gradients T_{ij}, we need their derivatives with respect to time $\dot{T}_{ij}$. This involves a knowledge of the velocity of the aircraft which is only approximately known because the measured values contain the influence of the anomalous gravity field. Therefore, an iterative solution will be advantageous in practical computations. The formulas for such a solution are also given in Moritz (1975)

$$v_i(t) = u_i^o - \int_{t_o}^{t} f_i(s)ds \qquad 2.2$$

$$\bar{T}_i(t) = T_i^o + \int_{t_o}^{t} T_{ij}(s)v_j(s)ds \qquad 2.3$$

$$T_i(t) = \bar{T}_i(t) + \int_{s=t_o}^{t} \int_{r=t_o}^{s} T_{ij}(s)T_j(r)drds \qquad 2.4$$

where u_i are the three velocity components and the other notations are as defined in equation (2.1). Again all quantities are regarded as functions of time, i.e. the variables t, r, and s all refer to time and are only used to distinguish the integration variables unambigously from one another. The upper case ^{o} denotes the value of the function at some initial time t_o.

The procedure can now be read from the formulas. With initial values u_i^o and T_i^o given, we first compute the approximate velocity components v_i at time t. These values

differ from the exact velocity components $u_i(t)$ by the effect of the anomalous gravity field in the accelerometer output f_i. Assuming for a moment the gravitational effect to be absent, formula (2.3) would give us the exact result, i.e. the components of the gravity disturbance vector. Since this is not the case, we get the approximation $\bar{T}_i(t)$. Using this approximation in the integral term of equation (2.4) will give more accurate values $T_i(t)$ which again can be used in the same way. Convergence presumed, we will finally obtain the exact gravity disturbance vector. It should be noted that at the same time the exact velocity components $u_i(t)$ can be computed. The integral term in equation (2.4) has been called interaction term because it expresses the interaction between gravitation and inertia. The size of this term compared to $\bar{T}_i$ is important for the speed of convergence of the iterative procedure.

The integrations performed in equations (2.2) to (2.4) are all along the flight path. From practical considerations this is very advantageous because measurements can be restricted to a specified region and computations can be performed in real time. Difficulties as in Stokes' or Vening-Meinesz' integral formulas where global data coverage is required do not occur. A simple analogy from classical geodesy is the astrogeodetic determination of the geoid where the deflections of the vertical are also needed along a profile only, in order to compute the geoid along this profile. It is interesting, however, that an analogue to Stokes formula also exists for the radial second-order gradient T_{rr}. It has been derived in Moritz (1967)

$$T = \frac{R^2}{2\pi} \iint_\sigma T_{rr} S_1(\psi) d\sigma \qquad 2.5$$

where R is the mean radius of the earth, ψ is the spherical distance and $S_1(\psi)$ is an analogue to Stokes function and given by

$$S_1(\psi) = (2-6\sin^2\tfrac{\psi}{2})\ln(1+1/\sin\tfrac{\psi}{2}) - 3 + 6\sin\tfrac{\psi}{2} . \qquad 2.6$$

The integration in (2.5) has to be extended over the surface of the earth. A general use of this formula cannot be recommended because the effect of the remote zones is even stronger than in Stokes' formula. But if a good coverage of T_{rr}-values is given in a certain area and enough outside information is available from other sources, a method similar to that of Marsh and Vincent (1974) may be applied to compute the fine structure of the geoid in that area. Such a procedure would also allow interesting comparisons with the collocation procedure to be treated next.

So far, we have discussed the problem of separating gravitation and inertia without reference to the quantities we actually want to obtain by our computations. Usually, these quantities will be mean gravity values in blocks of specified sizes on the surface of the earth. To derive them from the measured or the integrated values, downward continuation and averaging procedures must be applied. This should be done in such a way that no relevant information of the measuring process is lost in the subsequent computations. This is difficult, however, with classical procedures. Taking as an example formulas (2.2) to (2.4), we will obtain the three components of the gravity disturbance vector T_ϕ , T_λ , T_r . Downward continuation of T_r , as that of Δg , does not involve T_ϕ or T_λ . Thus, valuable information is not used at all. Similarly, downward continuation of the T_{rr}-gradient would not make use of the four other independent second-order gradients. The situation becomes even more complicated if measurements from other sources which are of different type must be combined with the gradiometer data. Therefore, we need a method which permits the combination of heterogenous data in different altitudes and their downward continuation to ground level. To obtain mean values from point values an interpolation procedure must be available which uses information about the average behaviour of the quan-

tities involved.

Moritz (1971) has proposed to use least-squares collocation for this purpose. The computational formulas are very simple, namely

$$s = C_{sx} C_{xx}^{-1} x \qquad 2.7$$

and

$$E_{ss} = C_{ss} - C_{sx} C_{xx}^{-1} C_{sx}^{T} \qquad 2.8$$

where s, the signal, is the quantity to be estimated, e.g. gravity anomalies; x is the vector of observations, e.g. second-order gradients, deflections of the vertical, gravity anomalies, height anomalies; C_{sx} is the covariance matrix connecting signal and observations; C_{xx} is the autocovariance matrix of the observations; C_{ss} is the autocovariance matrix of the signal. Given a number of observed values and an appropriate covariance function, the signal quantities s and their error covariance matrix E_{ss} may be estimated from formulas (2.7) and (2.8). Since we are interested in accuracy estimates only formula (2.8) will be used in the sequel.

The concept of a covariance function plays a decisive role in the collocation method. Therefore it will be discussed in detail in section 3 and we can restrict ourselves to some more general remarks at this point. Basically, the covariance function supplies information on the structure of the gravity field. As all measured quantities belong to the same gravity field and are related by functional equations, it is possible, under certain assumptions, to derive their different covariance functions from one basic function. This is the reason why the estimation by formuals (2.7) and (2.8) can combine heterogenous data in a consistent way. Furthermore, the basic covariance function can be selected in such a way that it can be analy-

tically continued down to sea level and all difficulties usually encountered in downward continuation can be avoided. Interpolation and downward continuation are then solved by the same algorithm. The information on the different altitudes is contained in the covariance function since the height difference is one variable of this function. The estimation of mean values is also possible by means of the covariance function. The averaging process is applied to the covariance function itself, changing the point anomaly function to a mean anomaly function, and again the algorithm of formulas (2.7) and (2.8) is applicable. If measuring errors must be taken into account this can be achieved by adding their effect to the autocovariance matrix of the measurements. Thus, all the different steps can be performed by appropriate changes of the covariance function, making the estimation of mean values from point values of heterogeneous data in different altitudes a single step procedure. This makes the method so attractive for applications.

Besides the signal which can be regarded as a stochastic quantity systematic effects may be taken into account. The corresponding formulas are

$$X = (A^T C_{xx}^{-1} A)^{-1} A^T C_{xx}^{-1} x \qquad 2.9$$

$$s = C_{sx} C_{xx}^{-1} (x - AX) \qquad 2.10$$

$$E_{XX} = (A^T C_{xx}^{-1} A)^{-1} \qquad 2.11$$

$$E_{ss} = C_{ss} - C_{sx} C_{xx}^{-1} C_{sx}^T + C_{sx} C_{xx}^{-1} A E_{XX} A^T C_{xx}^{-1} C_{sx}^T \qquad 2.12$$

where X are the systematic parameters to be estimated, A is the coefficient matrix of the parameters, and E_{XX} is their error covariance matrix. Simplifications of these formulas are possible in special cases, see Schwarz (1974).

3. Choice of a Covariance Function.

It has been pointed out that in least-squares collocation the information on the structure of the gravity field is supplied by the covariance function. The determination of such a function from empirical data is usually governed by two viewpoints. On the one hand the covariance function should represent certain statistical properties of the gravity field as determined from the data; on the other hand it should be of a simple analytical form so that the necessary derivations can be performed in such a way as to secure computational efficiency. The second requirement has so far only been met by isotropic and homogeneous covariance functions, i.e. functions which are invariant with respect to rotations and translations. Therefore the following discussion will be restricted to these functions.

A question which arises naturally when fitting empirical data to some kind of model function is: how many parameters are essential for the model function? This question has recently been studied by Moritz (1976) for isotropic and homogeneous covariance functions in the plane which can be extended into outer space. He has shown that rotationally symmetric harmonic covariance functions in space usually have planar equivalents and that results obtained for the planar approximations carry over to the spherical case with only small modifications. These results will be used in the sequel.

In Moritz (1976) three essential parameters are given for a covariance function $C(s)$: the variance C_o , the correlation length ξ , and the curvature parameter χ . Their geometrical interpretation is given by fig. 3.1. The variance C_o is the value of the covariance function $C(s)$ for the argument $s = 0$

$$C_o = C(0) \ . \qquad 3.1$$

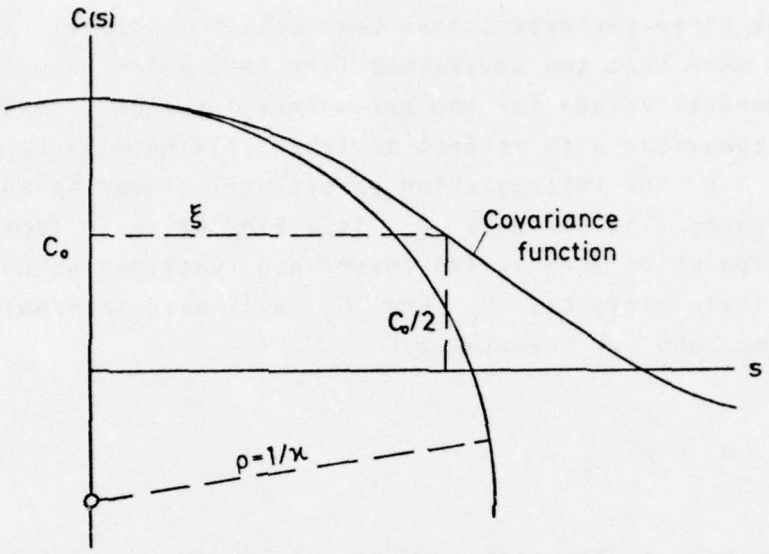

Fig. 3.1 Geometrical interpretation
of essential parameters

The correlation length ξ is the value of the argument for which

$$C(\xi) = C_o/2 \ . \qquad 3.2$$

The curvature parameter χ is related to the curvature of the covariance curve at $s = 0$ by

$$\chi = \kappa\xi/C_o \ . \qquad 3.3$$

where κ is the curvature. If we norm the covariance curve by setting $C_o = 1$ and $\xi = 1$ we obtain

$$\bar{\chi} = \kappa \qquad 3.4$$

which explains the name chosen.

The three parameters have been called essential. This does not mean that two covariance functions which have the same numerical values for the parameters are equal. But their general behaviour with respect to interpolation will be very similar, i.e. the interpolation errors will almost be the same in both cases. The variance C_o is a kind of scale factor for the interpolation errors. Two covariance functions which differ only in their variances C_1 and C_2 will have interpolation errors m_1 and m_2 related by

$$m_1^2 = \frac{C_1}{C_2} m_2^2 \quad . \qquad 3.5$$

Relations between the other parameters cannot be put into such a simple form but it can generally be said that χ characterizes the behaviour of the covariance function for small distances s, while ξ describes the behaviour for distances on the order of ξ itself. This indicates that the shape of the covariance curve at distances larger than about $1.5\,\xi$ is not very decisive, a fact which is confirmed by numerical computations. On the other hand a realistic choice of χ is very important because the curvature at the origin influences the interpolation for small distances. A model which is only fitted to C_o and $C(\xi)$ may produce a strongly distorted picture of the actual covariance behaviour. It can e.g. be shown that for a reasonable overall fit of the empirical gravity anomaly covariance function, the variance G_o of the horizontal gradients of Δg may differ by a ratio of 1:30 depending on the model chosen. Since this variance is related to the curvature parameter χ by

$$G_o = \chi \cdot C_o / \xi^2 \quad , \qquad 3.6$$

see (Moritz, 1976, p.25), the necessity of a third essential parameter is quite evident. In practice, the curvature at the

the origin is usually not very well known from empirical data. On the other hand, the variance G_o is more accessible to statistical estimation. It is therefore advisable to select the basic covariance model using G_o as the third parameter. The curvature parameter χ may then be determined by

$$\chi = G_o \cdot \xi^2 / C_o \quad . \tag{3.7}$$

Thus, we will regard C_o, ξ, and G_o as the three essential parameters in the sequel.

As can be seen from this example the choice of an adequate covariance model is influenced by the amount and type of empirical data available. Presently, good statistical information on some important parameters is lacking. Furthermore, none of the covariance models proposed so far will fit all empirical data equally well. Probably this can only be achieved by combining different models. It seems therefore reasonable to distinguish global and local applications at this point. It must be stressed, however, that this distinction is purely from practical reasons. In global applications a good fit to the covariance function of mean gravity anomalies of certain block sizes and to the low degree-variances as determined from satellites is satisfactory. In local applications a good fit to a point anomaly function and to the variance of its gradients is necessary. It is therefore not advisable to derive local covariance functions from a global function determined in the above way. Mean gravity anomalies do not contain reliable information on the curvature parameter of the corresponding point covariance function. If the variances C_o or G_o are fitted to their empirical values afterwards the incorrect information is already part of the model and will influence all subsequent computations. Consequently, the parameters essential for a local covariance function must already be considered when selecting the model.

In the following only local covariance functions are discussed because the use of gradiometer data makes a realistic local behaviour much more important than a good global fit. Therefore, we need as essential parameters the variance C_o of the point gravity anomalies, the correlation length ξ of the corresponding covariance function and the variance G of the horizontal gradients of the gravity anomalies. Furthermore, since aerial gradiometry has important advantages when applied over sea, differences in the gradient behaviour over sea and over land should be considered. As a typical example we will regard a sea surface area with depth between 3 and 6 km. This depth range covers more than 50 % of the surface of the earth, i.e. more than 70 % of the total sea surface.

Representative covariance functions of point gravity anomalies have not been published in the last decade; the careful investigations of Tscherning and Rapp (1974) have been devoted to a covariance function from $1^\circ \times 1^\circ$ mean gravity anomalies, and the point anomaly function derived from it will not be used here for reasons mentioned above. Therefore, the basic material to obtain estimates for C_o and ξ has been taken from publications of Hirvonen (1962) and Kaula (1966). Hirvonen's covariance function is a purely local one determined from 12 samples (area $1^\circ \times 1^\circ$) in the state of Ohio. Kaula's covariance function is more representative coming from 9 local (area $2^\circ \times 2^\circ$) and 8 regional samples (area $10^\circ \times 10^\circ$), half of them ocean areas. Using these empirical data, two local covariance functions will be derived which should be different enough to realistically cover the range of possible functions. The information needed in the sequel is summarized in table 3.1:

Covariance function	Estimated from areas of size	Number of areas	C_o (mgal^2)	ξ (km)
Hirvonen	$1^\circ \times 1^\circ$	12	337	40
Kaula	$2^\circ \times 2^\circ$ $10^\circ \times 10^\circ$	9 8	1201	83

Table 3.1 Information on empirical covariance functions.

A reliable estimate of the variance G_o is difficult to get. The values found in different publications vary between 30 E^2 and 330 E^2 for the horizontal gradients of Δg, where

$$1\ E = 10^{-9}\,\mathrm{sec}^{-2} = 0.1\ \mathrm{mgal/km}\ .$$

Most of these values are not very representative because sample sizes are small and are taken from one area only. Furthermore, all of them are from terrestrial measurements and are influenced by topographical effects. Sea surface gradients for the given depth range will probably have a much smoother behaviour than their terrestrial equivalents. There is another reason why for aerial gradiometry the parameter G_o may be expected close to the lower limit of the above estimates. The measurements are not actually point values but mean values at intervals of 10 sec, i.e. at a distance of about 2.6 km for a flying speed of 500 knots. Naturally, these mean values will be smoother than point values. Assuming therefore

$$30\ E^2 \leq G_o \leq 200\ E^2\ , \qquad 3.8$$

we obtain from table 3.1 and formula (3.3)

$$1.4 \leq \chi_1 \leq 8.5 \qquad 1.7 \leq \chi_2 \leq 10.8 \qquad 3.9$$

where the indices 1 and 2 refer to the Hirvonen and the Kaula estimates respectively.

With estimates for the three essential parameters given, we can select a covariance model which will meet the requirements. A rotationally symmetric harmonic covariance function in space can be expressed in the general form

$$K(P,Q) = A \sum_{n=o}^{\infty} k_n \left(\frac{R_B^2}{r_P r_Q}\right)^{n+1} P_n(\cos\psi) \qquad 3.10$$

where P and Q are two points in space with radius vectors r_P and r_Q respectively, ψ is the angle between r_P and r_Q, R_B is the radius of some sphere - frequently called the Bjerhammar sphere - completely inside the mean terrestrial sphere (R = 6371 km), $P_n(\cos\psi)$ are the Legendre polynomials, and k_n are positive coefficients. We will use the substitution

$$s = \frac{R_B^2}{r_P r_Q} \quad , \tag{3.11}$$

since no confusion with the distance variable s can occur in the sequel and we obtain

$$K(P,Q) = A \sum_{n=0}^{\infty} k_n s^{n+1} P_n(\cos\psi) \quad . \tag{3.12}$$

Different models of the covariance function can be obtained by defining k_n in different ways. Some of them are given in table 3.2:

Name	k_n	χ of planar equivalent
Reciprocal Distance C.F.	1	3.00
Poisson C.F.	2n + 1	1.76
Logarithmic C.F., type 1	1/n	variable
" " , type 2	1/(n-1)(n-2)	"
" " , type 3	1/(n-1)(n-2)(n+B)	"

Table: 3.2: Covariance function models according to equation (3.11).

The names have been taken from Moritz (1976) where also the determination of the curvature parameter χ for each function is discussed in detail. The logarithmic covariance models of

type 2 and type 3 have been used by Tscherning and Rapp (1974) to obtain a global covariance function from empirical data. The reciprocal distance covariance function and the Poisson covariance function have already been considered by Krarup (1969). Since the information on the empirical χ-values is only given in a certain range it seems advisable not to use the first two models because we may force the data by keeping a fixed value for χ. On the other hand, we may arrive at unrealistically large χ-values when using one of the logarithmic covariance functions (see Moritz, 1976, p.48).

Let us therefore first consider the parameters in equation (3.12) and their relation to the three essential parameters C_o, ξ, and $\chi(G_o)$. The value of $K(P,Q)$ can be varied in three ways once the model for the coefficients k_n has been selected. We can change the values of A and s on the right-hand side of equation (3.12), and we can substract a certain number of coefficients k_n. A change of A will only change the scale of the covariance function, i.e. A is directly related to C_o. If s becomes smaller, the covariance curve flattens out, i.e. ξ becomes larger and C_o becomes smaller. Since G_o decreases even more rapidly than C_o, the parameter χ stays almost constant for the logarithmic covariance function of type 2 and decreases for type 3. If we subtract the first m coefficients k_n the covariance curve becomes steeper and the parameters ξ, C_o and χ become smaller. The value of G_o does not change very much as long as we stay in the low frequency range. This shows that the local character of the second-order gradients is well represented by these models. In the practical determination it is most important to determine first an appropriate range of values for s, because we may otherwise obtain unrealistic values for G_o and χ. This can best be done by fixing the ratio $C_o : G_o$ because it is most sensitive to changes in s. Thereafter, ξ can be fitted by subtracting a certain number

of coefficients and finally the function is scaled by selecting an appropriate value for A. Table 3.3 shows the interplay between C_o, G_o, ξ, χ and s.

s	Logarithmic cov.fct., type 2			Logarithmic cov.fct., type 3		
	$C_o:G_o$	ξ	χ	$C_o:G_o$	ξ	χ
0.999	0.4:1	11.2	3.02	2.7:1	70.2	18.12
0.998	1.6:1	22.2	3.03	9.0:1	103.2	11.93
0.997	3.6:1	33.4	3.04	17.8:1	130.0	9.49
0.996	6.5:1	44.6	3.05	28.8:1	153.8	8.21
0.995	10.2:1	55.8	3.06	41.8:1	174.7	7.31
0.994	14.7:1	67.1	3.07	56.3:1	197.6	6.93
0.993	19.9:1	78.3	3.07	72.5:1	216.3	6.45
0.992	26.0:1	89.5	3.08	90.2:1	234.6	6.10

Table 3.3 Covariance models and essential parameters.

The best estimate of a global point gravity anomaly variance is the value $C_o = 1795$ mgal^2 determined by Tscherning and Rapp (1974). Using table 4 of that publication, we get a somewhat lower $C_o = 1576$ mgal^2 for ocean areas in the 3 to 6 km depth range. To get an estimate comparable to Kaula's sampling areas we have to subtract the influence of the low frequencies with half range larger than 10°. Using satellite derived coefficients, we get values of about 1590 mgal^2 and 1375 mgal^2 for the above estimates. Thus, $C_o = 1500$ mgal^2 has been chosen as a round value for a covariance function of Kaula type. The effect of a change in the variance C_o on the mean square error can then easily be computed by formula (3.5). Considering the inequality (3.8), the ratio $C_o : G_o$ should be about 10:1 to 15:1. Using this ratio to fix the range of s, the correlation length ξ and the scale of the covariance function have been determined in the way described above.

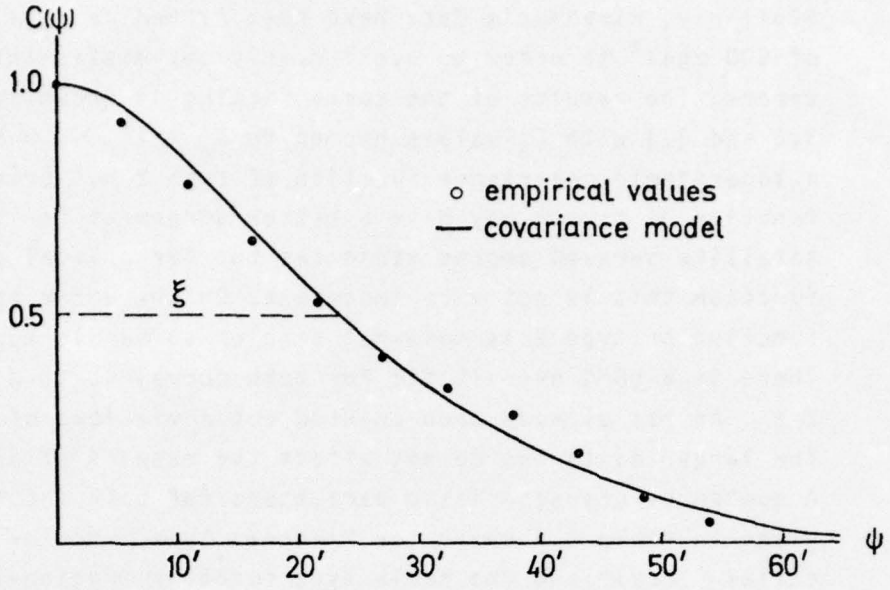

Fig.3.2 Fit to Hirvonen's empirical covariances.

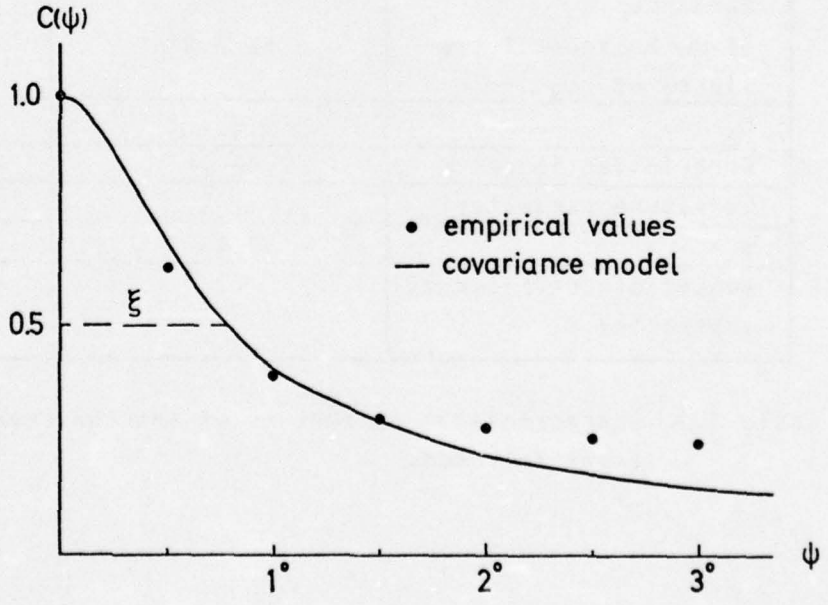

Fig.3.3 Fit to Kaula's empirical covariances.

Similarly, Hirvonen's data have been fitted using a C_o-value of 500 $mgal^2$ in order to avoid overly optimistic interpolation errors. The results of the curve fitting is shown in figures 3.2 and 3.3 with C_o-values normed to $C_o = 1$. In both cases a logarithmic covariance function of type 2 has been used. A function of type 3 may give a better agreement for the low satellite derived degree variances but for a local covariance function this is not very important. On the other hand, a function of type 2 is somewhat simpler to handle numerically. There is a good overall fit for both curves up to distances of 2 ξ . As has already been pointed out deviations of the curves for larger distances do not affect the results of interpolation. A number of characteristic parameters for both functions are given in table 3.4 where the Hirvonen type function has been called "local" and the Kaula type function "regional".

Parameter	Local covariance function	Regional covariance function
Variance of gravity anomalies C_o	500 $mgal^2$	1500 $mgal^2$
Variance G_o of the horizontal gradients of Δg	52.5 E^2	111.4 E^2
$C_o : G_o$	9.5 : 1	13.5 :1
Correlation length ξ	43 km	61 km
Curvature parameter χ	1.9	2.8
s =	0.994	0.994
Number of coefficients subtracted	70	12

Table 3.4 Characteristic parameters of the two covariance functions selected.

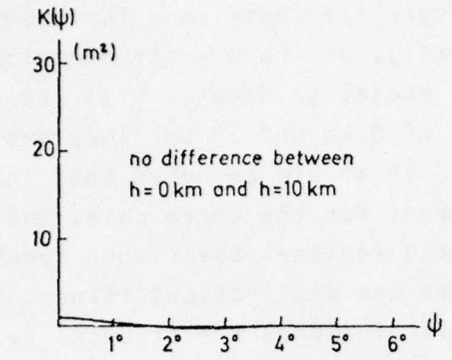

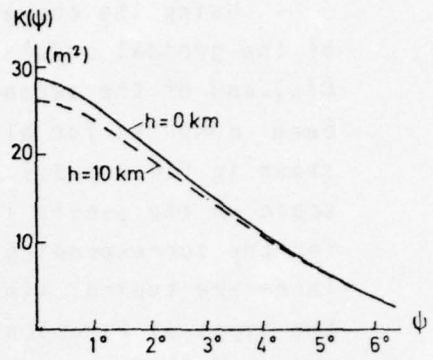

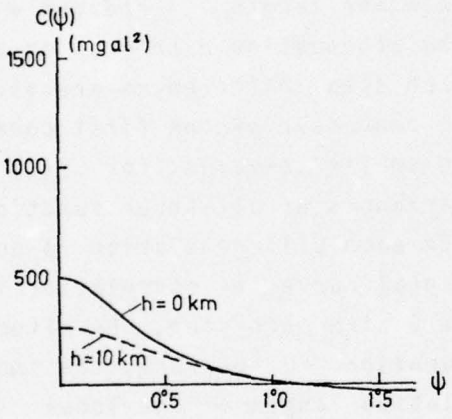

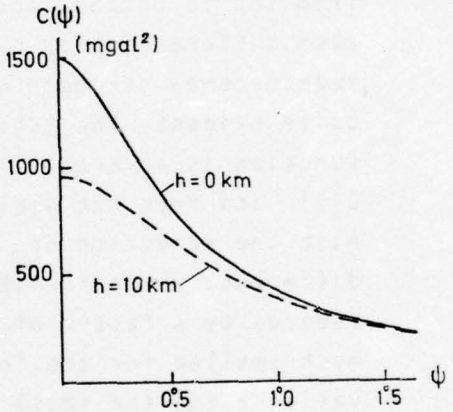

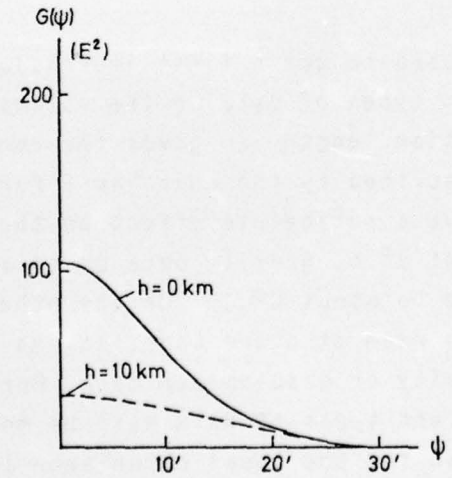

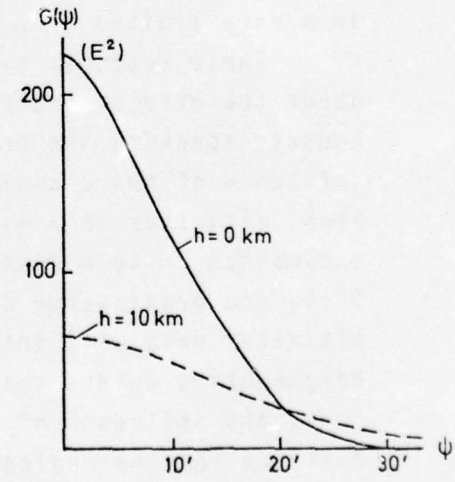

Fig.3.4 Local covariance function.

Fig.3.5 Regional covariance function.

Using the above parameters the covariance functions of the geoidal undulations $K(\psi)$, of the gravity anomalies $C(\psi)$, and of the second-order radial gradients $G(\psi)$ have been computed for altitudes of 0 km and 10 km. They are shown in figures 3.4 and 3.5. It should be noted that the scale on the ψ-axis is different for the three cases but equal for the corresponding local and regional covariance functions. There are typical similarities and distinctions between the two types of functions. Similar features are produced by the order of differentiation which in fig. 3.3 and 3.4 increases from top to bottom. The correlation length ξ reduces with each differentiation while the attenuation with growing altitude becomes stronger with each step. Differences are also quite evident. The more local character of the first covariance function is apparent from the smaller ξ-values for $K(\psi)$ and $C(\psi)$ and from the smaller variances of all three functions. Also the reduction of ξ with each differentiation is quite different. While for the regional curve the correlation length reduces by a factor of almost 5 with each step, the effect is much smaller for the local function. Furthermore, the small variance and the small correlation length of the local $K(\psi)$-function indicate that the variation of the geoid is considered in a very limited area only.

These features can be used to get a first impression about the effect of different types of data on the estimation. Loosely speaking the correlation length ξ gives the zone of influence of the quantity described by the covariance function. Thus, altimeter data will have a noticeable effect on the estimation up to a distance of $3^{\circ}.5$, gravity data up to about $0^{\circ}.6$, and gradiometer data up to about $0^{\circ}.15$. On the other side, altimeter data will introduce much stronger correlations between neighbouring points than gravity or gradiometer data. Furthermore, the influence of different types of data will be more distinct for the regional than for the local covariance function.

These features can advantageously be used for the combination of heterogeneous data and for the design of stable numerical procedures, although for a full assessment crosscorrelations have to be taken into account.

4. Interpolation at Flight level.

The first tentative conclusions drawn at the end of the preceding section will now be substantiated by detailed computations. The basic formula has already been given in section 2

$$E_{ss} = C_{ss} - C_{sx} C_{xx}^{-1} C_{sx}^{T} \quad . \qquad 4.1$$

The values to be estimated, the components of the signal s, are Δg-values in arbitrary positions between the profiles. E_{ss} is their error covariance matrix and the square roots of the diagonal terms of this matrix are the standard errors of the gravity anomalies. The measurements x used in this section are gradiometer data in a ϕ, λ, r-system and Δg-values obtained by integrating along the profile according to formulas (2.2) to (2.4). Mean values at intervals of 10 sec. are considered as gradiometer measurements. The elements of the covariance matrices are determined by applying functions similar to equation (3.12) for two specific points P and Q or, since we are using isotropic covariance functions, by introducing the spherical distance ψ between the two points and their respective heights. If measuring errors must be taken into account, the covariance matrix of the measurements C_{xx} has to be augmented by the covariance matrix of the noise C_{nn} and we shall write

$$C = C_{xx} + C_{nn} \qquad 4.2$$

so that formula (4.1) reads

$$E_{ss} = C_{ss} - C_{sx}C^{-1}C_{sx}^{T} \quad . \qquad 4.3$$

This formula will always be applied in the sequel for reasons of numerical stability as discussed in section 9. We have used standard errors of $\pm$ 1 mgal and $\pm$ 1 E for the gravity anomalies and the gradiometer data respectively. If we regard these errors as independent we have a C_{nn}-matrix of the form

$$C_{nn} = \sigma_i I \qquad 4.4.$$

where σ_i are the error variances of the different types of data and I is the unit matrix. Usually the differences between this model and pure interpolation with $\sigma_i = 0$ are negligible. If necessary, σ_i has been appropriately reduced.

It will first be investigated how the data can be combined in an optimal way. There are four obvious alternatives. Following the classical procedure we can regard Δg only and interpolate between the profiles. In this case a large part of the existing information is neglected. Next, the use of all three first-order gradients T_ϕ , T_λ , T_r will be considered, implying that the information of five independent gradiometer measurements can be condensed into three first-order gradients. Alternatively, we will use five second-order gradients only. Finally, a combination of Δg and different second-order gradients will be used. It should be noted that in all cases where integrated values are employed correlations via the measuring errors are introduced. A rigorous model should take these correlations into account. Since their influence is negligible as long as the error variances are small compared to the signal variances the simple error model (4.4) has been kept.

When considering formula (4.1) it can be seen that the inversion of the matrix C is the time-consuming part, numerically. The dimension of C is given by the number of measure-

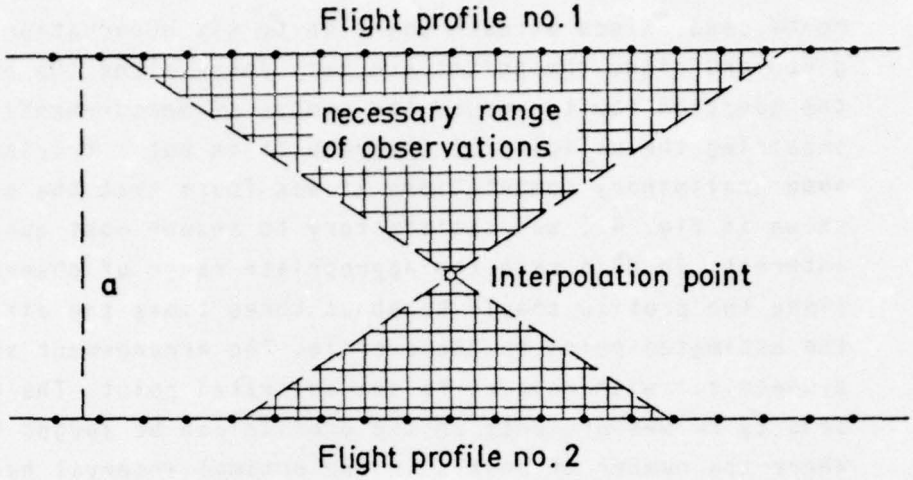

Fig.4.1 Basic configuration.

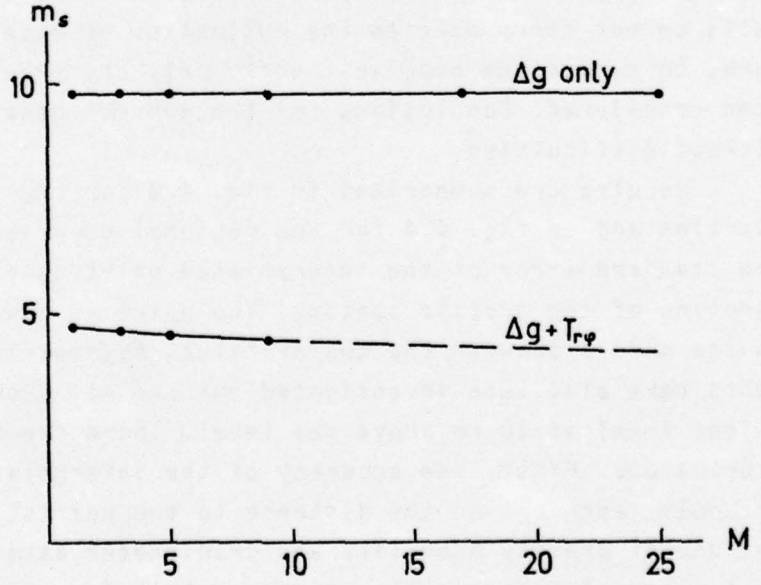

Fig.4.2 Interpolation error m_s as function of number of points M on each profile.

ments used. Since at each point up to six observations are given and since the points are very dense along the profile, the question how to reduce the number of measurements without impairing the validity of the results is not a trivial one. After some preliminary computations it was found that the arrangement shown in fig. 4.1 was satisfactory to answer most questions of interest. In this case the appropriate range of observations along the profile should be about three times the distance from the estimated point to the profile. The arrangement should be symmetrical with respect to the estimated point. The required density of measurements on the profile can be judged from fig.4.2 where the number of points in the optimal interval has been varied. As can be seen the standard errors decrease only slightly with an increasing number of points and even an arrangement with three points on each profile will bring reliable results. Thus, a dense sequence of points along the profile which is necessary when integrating first-order gradients, is not needed for interpolation purposes. It should be noted, however, that these results do not carry over to the estimation of mean values. Furthermore, to reduce the numerical work, only east-west profiles have been considered. Conclusions for the general case can be derived without difficulties.

Results are summarized in fig. 4.3 for the local covariance function and in fig. 4.4 for the regional covariance function. The standard error of the interpolated point is plotted as a function of the profile spacing. The point is always situated in the middle between the two profiles. Asymmetrical arrangements have also been investigated but are not shown here. The flight level is 10 km above sea level. There are two obvious conclusions. First, the accuracy of the interpolated point is strongly dependent on the distance to the nearest profile. Second, the use of gravity anomalies and gradiometer data will give the best interpolation results. A more detailed examination of the curves shows that results are very poor when using gradiometer data only. This indicates that we can only expect the fine

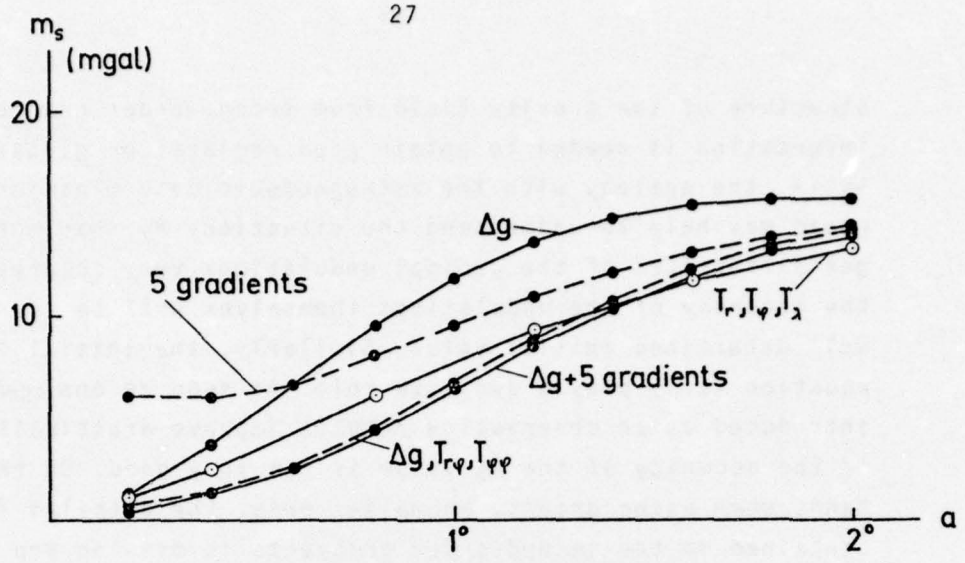

Fig.4.3 Local covariance function
Standard error of interpolation.

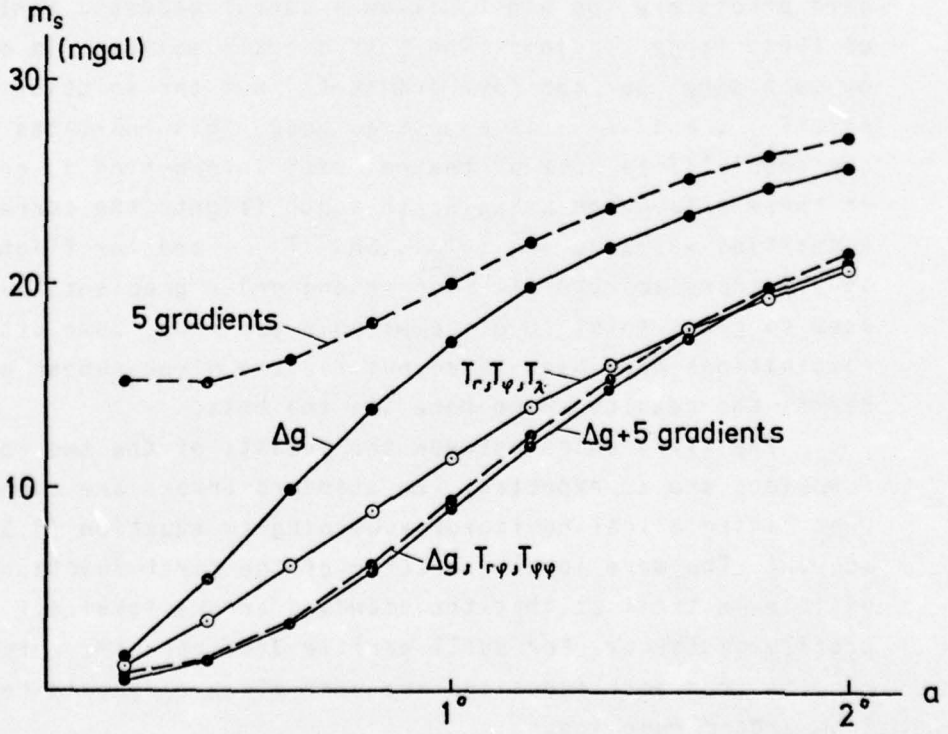

Fig.4.4 Regional covariance function
Standard error of interpolation.

structure of the gravity field from second-order gradients. More information is needed to obtain good regional or global values. Again, the analogy with the astrogeodetic determination of the geoid may help to understand the situation. By that method we get differences of the geoidal undulations very accurately but the accuracy of the undulations themselves will be poor without a well determined initial value. Similarly, the initial values in equation (2.3) play a decisive role. As soon as one Δg-value is introduced as an observation results improve drastically even if the accuracy of the Δg-value is not very good. On the other hand, when using gravity anomalies only, the detailed information contained in the second-order gradients is missing and the accuracy is significantly lower than in the combination solution. The same argument holds in case of the three first-order gradients for small profile spacings. For profile spacings larger than $1^{\circ}.5$ first-order gradients will give the best solution but standard errors are too big to allow a useful geodetic application of these large spacings. The best overall solution is obtained by combining Δg and five gradients. But the solution using Δg , $T_{r\phi}$, and $T_{\phi\phi}$ is almost as good. This indicates that in our special case most of the relevant information is contained in these data. When using north-south flights the corresponding quantities would be Δg , $T_{r\lambda}$ and $T_{\lambda\lambda}$, and for flights with an arbitrary azimuth all four second-order gradients must be used to get a solution of comparable accuracy. Some other data combinations have been tried but for the given number of gradients the results shown here are the best.

The differences between the results of the two covariance functions are as expected. The standard errors are comparable when taking a scaling factor according to equation (3.5) into account. The more local character of the first function is visible in the fact that the standard errors level off for large profile distances. For small profile distances the corresponding results from both functions are very close as should be expected from a good modeling.

5. Downward Continuation.

Downward continuation of gravity is an improperly posed problem and the numerical difficulties which arise when looking for an approximate solution have been described in Schwarz (1973). Downward continuation of second-order gradients is an even more sensitive process because the attenuation of the values with height is much stronger. For a detailed discussion of the spectral properties of such a process reference is made to Rummel (1975). The mathematical instability of the problem is eliminated in the collocation procedure by selecting a covariance function that can be analytically continued down to sea level. In this way downward continuation can be regarded as a problem of spatial interpolation. The numerical instability, i.e. the possibility that the resulting covariance matrix is close to an ill-conditioned one, is controlled by using a formula of type (4.3) where the diagonal of the matrix to be inverted is augmented by small amounts. Thus, there is no change in the numerical procedure compared to the preceding section. The transition from a plane to a spatial covariance function will only be visible in the covariance matrices C_{ss} and C_{sx} because the signal is now at ground level (h = 0 km) while the measurements remain at flight level (h = 10 km).

Again, some computations have been made to determine the range and the density of the observations. Results are similar to those of the preceding section and no change in the basic design is necessary. As can be seen from figures 5.1 and 5.2 spatial interpolation follows the same pattern as planar interpolation if the flying altitude is small compared to the profile spacing. Again, the accuracy of an interpolated point is dependent on the distance to the closest observation point and the solutions combining Δg-values and gradiometer data will give the best results. Again, for east-west profiles the combination of Δg , $T_{r\phi}$, and $T_{\phi\phi}$ is very close to the optimal

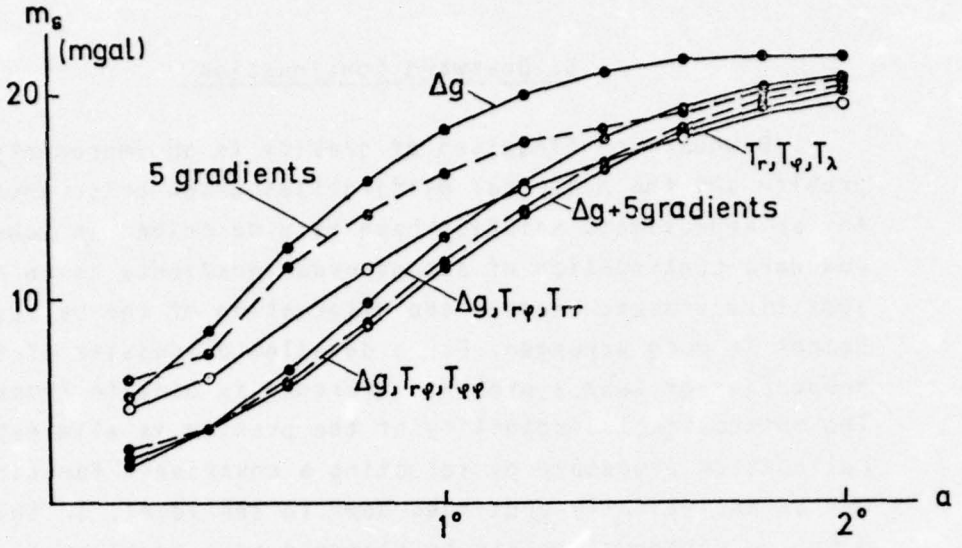

Fig.5.1 Local covariance function
Standard error of downward continuation.

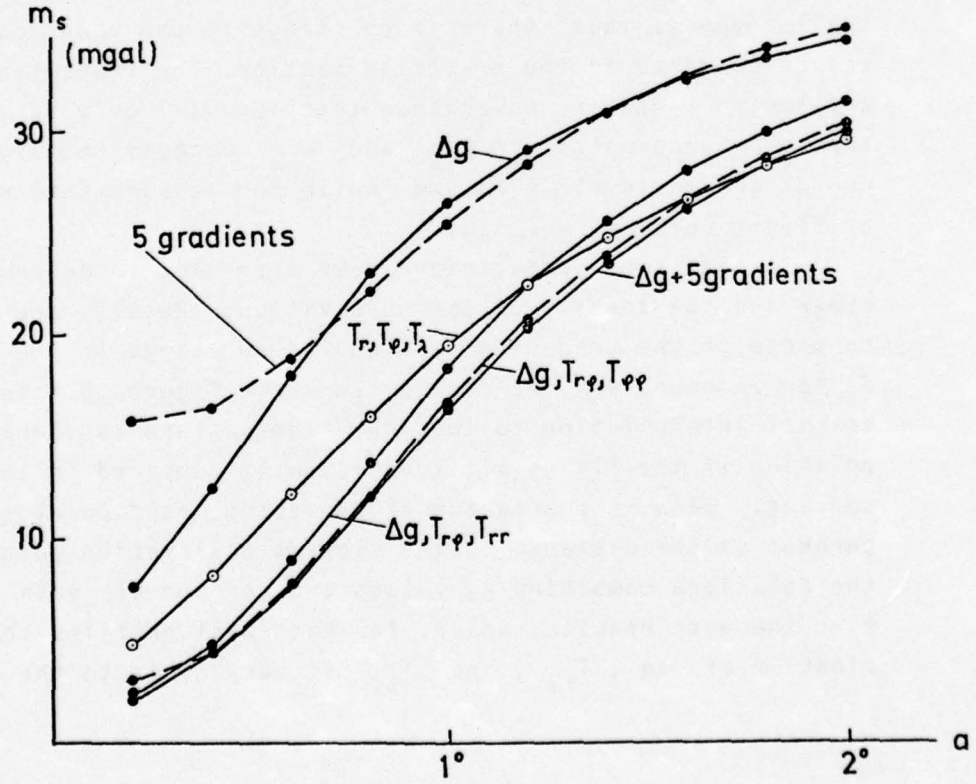

Fig.5.2 Regional covariance function
Standard error of downward continuation.

solution. However, for profile spacings smaller than about $0^{\circ}.35$ the combination of Δg , $T_{r\phi}$, and T_{rr} gives better results. This shows that the high resolution of the T_{rr}-gradients will only be effective in a limited area below the measuring point. For blocks of small size this can advantageously be used because it will not only give a better accuracy but also reduce the correlation between neighbouring points. If the point to be interpolated is directly below the flight path, the combination of Δg , $T_{r\lambda}$, and $T_{\lambda\lambda}$ for a wide point spacing ($> 0^{\circ}.35$) and of Δg , $T_{r\lambda}$, and T_{rr} for a dense point spacing ($> 0^{\circ}.35$) will give the best results. For north-south profiles $T_{r\phi}$, $T_{\phi\phi}$ have to be replaced by $T_{r\lambda}$, $T_{\lambda\lambda}$ and vice versa to get the corresponding results.

Some experiments have been made with a different arrangement of profiles. If a constant spacing is kept, the addition of more profiles will affect the results only for spacings below $0^{\circ}.3$, i.e. if the ratio between profile spacing and flying altitude is smaller than 3:1. Even then, the effect will not be very marked, so that the results presented in figures 5.1 and 5.2 are fairly general. The use of a grid of east-west and north-south profiles has also be considered. With a fixed number of flights the spacing of the profiles for the grid system will be much wider than for profiles in one direction and the interpolation accuracy will be worse in this case. Therefore, cross profiles should only be used for updating purposes.

For further reference the main results of the last two sections are summarized:

a.) The accuracy of an interpolated point is mainly dependent on its distance to the nearest profile. Therefore, a dense profile spacing is more important for the accuracy of interpolation than cross profiles.

b.) The dense sequence of points along the profiles, necessary when integrating first-order gradients, is not needed for interpolation purposes. A density between a/4 and a/2, where a is the profile spacing, will usually be sufficient.

c.) For profiles with arbitrary azimuth an optimal data combination should include:

Δg , $T_{r\phi}$, $T_{r\lambda}$, $T_{\phi\phi}$, $T_{\lambda\lambda}$ for profile spacings larger than $0^{\circ}.3$.

Δg , $T_{r\phi}$, $T_{r\lambda}$, T_{rr} for profile spacings smaller than $0^{\circ}.3$.

The inclusion of more second-order gradients will only slightly improve the accuracy but may add to the numerical problems. A smaller number of gradients may be used in special cases.

6. Influence of Measuring Errors.

It has been mentioned in the introduction that the results of this accuracy study hinge on realistic assumptions about the structure of the gravity field and the accuracy of the measurements. At the moment no airborne gradiometer is in operation and therefore realistic estimates are difficult to obtain. It is expected that the instruments will give a standard error of $\pm$ 1 E for any component integrated over an interval of 10 sec. Gravity values at flight level can be obtained by integrating the gradiometer values along the flight path. Moritz (1975) has studied the error propagation of Δg along a profile under certain simplifying assumptions. The standard error of Δg is dependent on the length of the profile and varies between $\pm$ 1.4 mgal for a distance of 100 km and $\pm$ 4.3 mgal for a distance of 1000 km when using the above standard error for the gradiometer data. Accurate initial values and a negligible influence of the interaction term are assumed in this case. Thus, a value of $\pm$ 1 mgal can be regarded as a fairly optimistic estimate for the standard error of the measurements. Actual errors may be considerably larger.

In order to get an idea about the sensitivity of the Δg-estimation with respect to errors in the different measurements, the standard errors for each type of data have been varied separately. Again, formula (4.3) can be used. The variances σ_i in equation (4.4) are the quantities which must be changed in

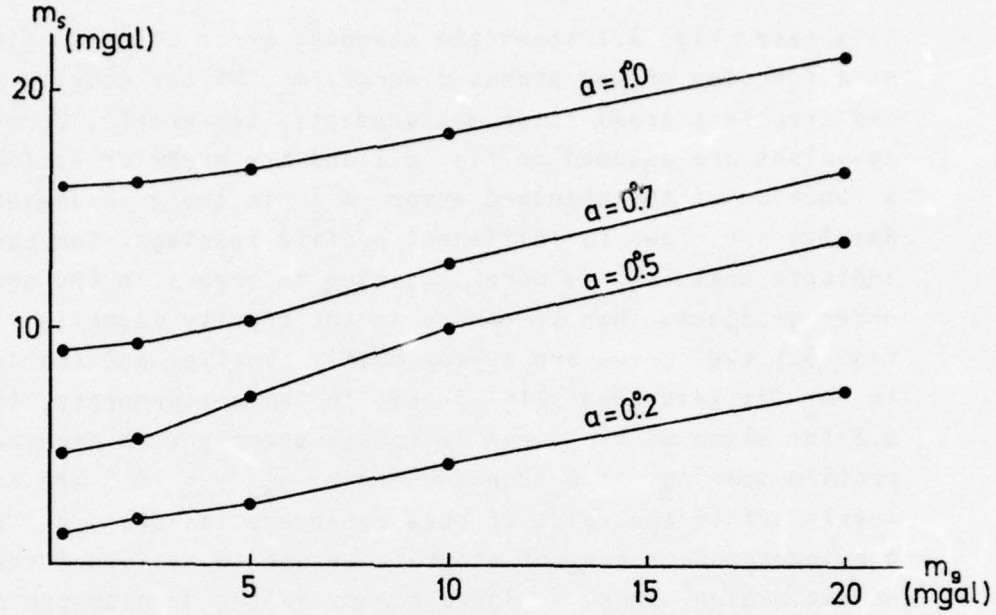

Fig.6.1 Influence of error in gravity anomalies (m_g).

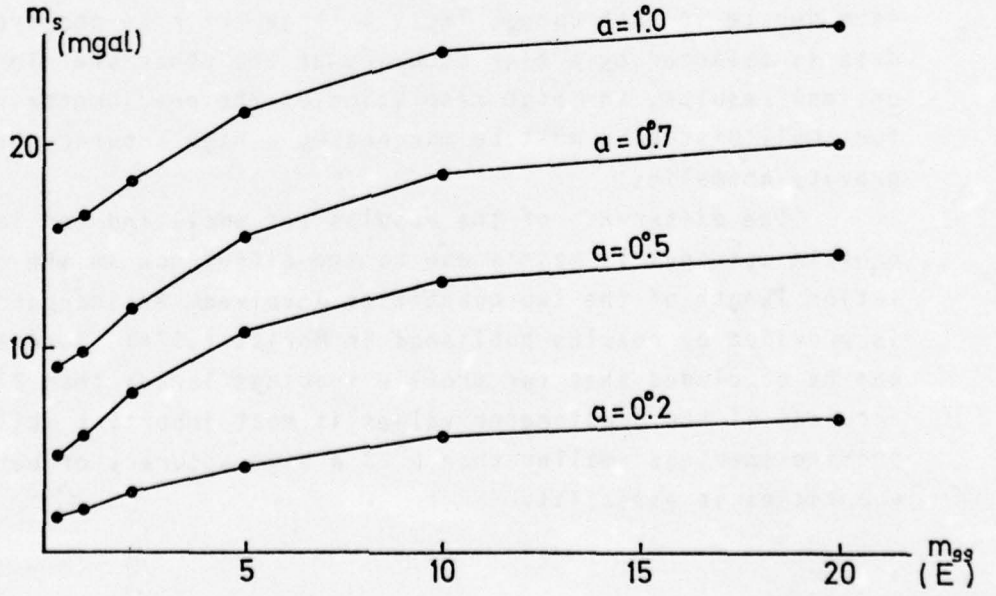

Fig.6.2 Influence of error in gradiometer data (m_{gg}).

this case. Fig. 6.1 shows the standard error of estimation m_s as a function of the standard error m_g of the gravity anomalies and errorless gradiometer measurements. Conversely, errorless Δg-values are assumed in fig. 6.2 and the error of estimation is a function of the standard error m_{gg} in the gradiometer data. Results are shown for different profile spacings. The curves indicate that m_s is more sensitive to errors in the second-order gradients than to errors in the gravity anomalies. In fig. 6.1 the curves are approximately parallel and the increase in m_s is less than half of that in the measurements. In fig. 6.2 the slope of the curve increases sharply with growing profile spacing. At a standard error $m_{gg} = \pm 10$ E the curve levels off to the value of pure Δg-interpolation, i.e. the gradiometer data are not accurate enough to influence the error of estimation. Thus, a high accuracy in the gradiometer data will control even a large error in Δg, while large errors in the second-order gradients usually cannot be balanced by highly accurate gravity anomalies.

The situation is somewhat different for small profile spacings. Here the increase in the standard error of estimation is moderate in both cases. Thus, a large error in one type of data is balanced by a high accuracy of the other one. To obtain optimal results, the high resolution of the gradiometer values for small distances must be matched by a high accuracy of the gravity anomalies.

The difference of the results for small and for large profile spacings is mainly due to the difference in the correlation length of the two quantities involved. An independent check is provided by results published in Moritz (1974). Generally, it can be concluded that for profile spacings larger than $0^\circ.3$ the accuracy of the gradiometer values is most important while for profile spacings smaller than $0^\circ.3$ a high accuracy of both quantities is essential.

7. Mean Values.

So far we have only considered the determination of point gravity anomalies. Usually mean values for blocks of specified size are required. The modifications of the basic formula (4.3) for this case are discussed in this section.

Meissl (1971) has shown how to derive a mean anomaly covariance function from a point anomaly covariance function by using a narrow-sense smoothing operator. Such an operator is defined by the properties $\lambda_n \to 0$ and $\lambda_o = 1$, where λ_i are the eigenvalues of the operator. The averaging operator over a circular cap of the sphere with angular radius ψ_o is an operator of this kind. Its eigenvalues are given by

$$\beta_n = \frac{1}{1-\cos\psi_o} \int_{\cos\psi_o}^{1} P_n(t)dt \qquad 7.1$$

or by the recurrence relation

$$\beta_n = \frac{1}{1-\cos\psi_o} \frac{1}{2n+1} \{P_{n-1}(\cos\psi_o) - P_{n+1}(\cos\psi_o)\}. \qquad 7.2$$

Replacing a block of rectangular form by a circular cap of equal area we can compute a mean anomaly covariance function by applying the smoothing operator to the point covariance function. Since in equation (3.12) we have the spectral representation of the point anomaly covariance function and in equation (7.1) the eigenvalues of the smoothing operator we can directly write

$$\bar{\bar{K}}(P,Q) = A \sum_{n=o}^{\infty} \beta_n^2 k_n s^{n+1} P_n(\cos\psi) \qquad 7.3$$

where $\bar{\bar{K}}(P,Q)$ is the mean anomaly covariance function derived from $K(P,Q)$. Blocks of different sizes will produce different

sets of β_n-values. In this way, we can check once more the model covariance function against empirical values. Taking e.g. the regional covariance function with all coefficients we get a variance of $C_o = 311\ \text{mgal}^2$ for $5^\circ \times 5^\circ$ blocks and a variance of $C_o = 996\ \text{mgal}^2$ for $1^\circ \times 1^\circ$ blocks as compared to $302\ \text{mgal}^2$ and $996\ \text{mgal}^2$ from empirical data. Although such a comparison is not very sensitive with respect to the local behaviour of the covariance function, it gives a good check on its global validity.

For all practical purposes the infinite series in equation (7.3) can now be replaced by a finite series. For a certain number N the terms $n > N$ will not contribute significantly to the value of the covariance function. Evidently, the smoothing property will be stronger for large blocks, i.e. the number N will be smaller for the covariance function of $5^\circ \times 5^\circ$ blocks than for $1^\circ \times 1^\circ$ blocks. Table 7.1 shows the number of necessary coefficients for different block sizes. N has been determined such that the terms $n > N$ will not change the integer values of the covariance function.

Block size	5' x 5'	15' x 15'	$1^\circ \times 1^\circ$	$5^\circ \times 5^\circ$
N	3000	1200	400	200

Table 7.1 Number of necessary coefficients β_n for different block sizes.

But even with a limited number of coefficients the actual summation of the series (7.3) will usually cost too much computer time. It would be advantageous if we could replace the infinite series (7.3) by a closed covariance expression as it can be done for the series (4.3). This is not possible with the β_n-values as defined by formula (7.1). We will therefore try to replace these coefficients by quantities which make such a summation feasible and are still close enough to the exact β_n-values.

Apparently it will be sufficient to have a good approximation for the range of values given in table 7.1 if $\beta_n \to 0$ can be secured for $n > N$. Keeping in mind that the β_n are only defined for integer values of n, we can represent them as in fig. 7.1 where the full line gives the β_n-curve for the $1^\circ \times 1^\circ$ blocks.

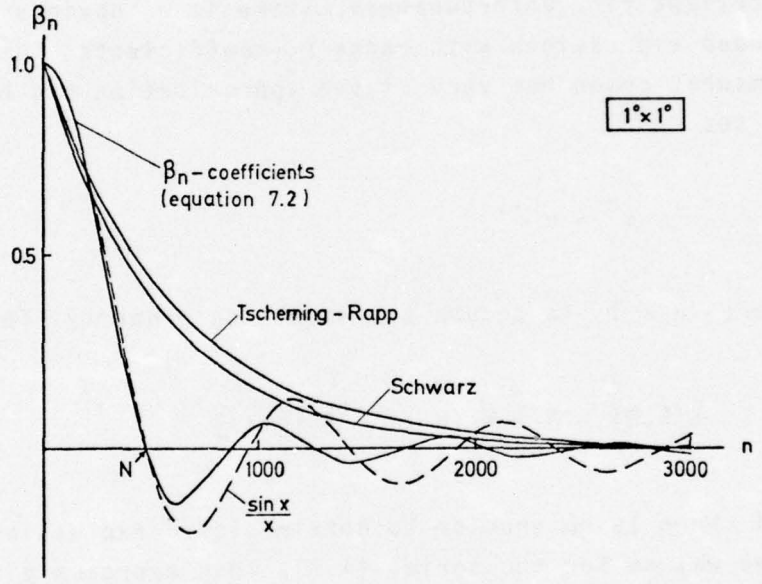

Fig.7.1 Smoothing coefficients β_n and approximations.

It is quite interesting that the first zero will roughly coincide with the number N given in table 7.1, i.e. that the oscillating β_n-values will not show up significantly in the covariances. This is true for all block sizes smaller than $2^\circ \times 2^\circ$. For $5^\circ \times 5^\circ$ blocks the oscillating part contributes about 1 %. Thus, for practical purposes it will be sufficient to approximate the β_n-curve up to its first zero by some other smoothing curve. A very good approximation of the β_n-values in the required range can be achieved by the function sinx/x where

$$x = \frac{\pi \cdot n}{N}$$

and N is the number of the coefficient closest to the first zero. In that case

$$\beta_n = \frac{N \sin(\pi \cdot n/N)}{\pi \cdot n} \quad , \qquad 7.4$$

and as can be seen from the dashed line in fig. 7.1 there is an excellent fit. Unfortunately, there is no obvious way to get closed expressions with these β_n-coefficients. Therefore, a somewhat crude but very simple approximation has been chosen. We set

$$\beta_n^2 = u^{n+1} \qquad 7.5$$

where $u < 1$ to secure the smoothing property. Then

$$\bar{K}(P,Q) = A \sum_{n=0}^{\infty} k_n (u\ s)^{n+1} P_n(\cos\psi) \qquad 7.6$$

and there is no problem to obtain closed expressions in the same way as for the series (4.3). This approach gives a simple interpretation of the averaging process. Because of $u < 1$ the radius of the Bjerhammar sphere is diminished to obtain the mean anomaly covariance function. This will result in smaller values C_o and G_o and in a larger correlation length ξ. Similarly, using the definition of s, equation (7.6) may be explained as an upward continuation of the original covariance function to a certain altitude without changing the radius of the Bjerhammar sphere. This interpretation has been used by Tscherning and Rapp (1974) and basically their method to obtain a mean anomaly covariance function is equivalent to equation (7.6). Because of this dual interpretation it can be expected that for a given block size the effects of downward continuation and of mean value determination will cancel at a certain altitude h.

Table 7.2 shows these altitudes for different block sizes.

Block size	$5^\circ \times 5^\circ$	$1^\circ \times 1^\circ$	15'x 15'	5' x 5'
u	.974153	.996234	.998884	.999951
h(km)	84	12	3.6	0.2

Table 7.2 Mean values and levels of upward continuation.

Take as an example the estimation of mean values of $1^\circ \times 1^\circ$ blocks at sea level. At a flight level of 12 km the effects of downward continuation and of mean value determination will cancel, i.e. they can be replaced by planar interpolation at h = 12 km. Usually it will not be feasible to fix flying altitudes in this way but the properties of a covariance function at a certain altitude may be appraised by comparing it to the corresponding mean value function. Taking as before h = 10 km, we can say that the Δg-values at this level will be almost as smooth as $1^\circ \times 1^\circ$ mean values on ground level. A very dense spacing of points will therefore increase correlations without essentially improving the accuracy of the results.

Fig. 7.1 shows two β_n-functions of type (7.6) as full lines. One has been used by Tscherning and Rapp (1974), the other one corresponds to the value u given in table 7.2. Both curves are only very crude approximations of the given function but the values of the corresponding mean anomaly covariance functions are very close to the exact ones. From the difference in the shape of the β_n-curve and that of the approximations it must be expected that the curvature parameter χ will be changed by the approximation. Therefore, the resulting covariance function should not only be compared for C_o but at least up to a spherical distance of $1.5 \cdot \xi$. This has been done for the β_n-values used in this report and the approximation is very close for the whole range. Thus, a more refined model for the β_n is not necessary

as long as mean gravity anomalies are considered. The situation will be quite different for mean values of the second-order gradients.

In order to apply formula (4.3) we still need the cross-covariance function between point and mean gravity anomalies $\bar{K}(P,Q)$. In analogy to formula (7.3) we may write

$$\bar{K}(P,Q) = A \sum_{n=0}^{\infty} \beta_n k_n s^{n+1} P_n(\cos\psi) \qquad 7.7$$

and with the approximation (7.5) we get

$$\bar{K}(P,Q) = A \sum_{n=0}^{\infty} k_n (\sqrt{u}\cdot s)^{n+1} P_n(\cos\psi) \ . \qquad 7.8$$

We then have

$$E_{ss} = \bar{\bar{C}}_{ss} - \bar{C}_{sx} C^{-1} \bar{C}^T_{sx} \qquad 7.9$$

for the estimation of mean values. Such a formula has e.g. been used by Lachapelle (1975) in the combination of gravimetric and astrogeodetic data. It should be noted, however, that some care must be taken when applying it. The estimation procedure expressed by formula (7.9) has still the main characteristics of an interpolation, i.e. the accuracy is dependent on the distance to the nearest profile. Therefore, the mean value should not be defined as the value at the centre of the block because otherwise the accuracy estimate will be misleading if e.g. a profile passes through the centre. Instead, a regular grid of points covering the area of the block can be used to determine the mean standard error. If properly chosen, the number of points must not be larger than about twice the number of profiles passing through the block.

Furthermore, the downward continuation problem can now be explained in a more penetrating way. The covariance function of the measurements at flight level is close to a mean anomaly covariance function of $1^\circ \times 1^\circ$ blocks. If we want to estimate mean values of smaller block sizes or even point values from these observations we must be aware of the fact that we are trying to reverse the averaging process. The results obtained in this way will be very smooth and strongly correlated. Thus, we cannot expect to recover the actual point values. Furthermore, it is well known that stability problems will arise in such unsmoothing procedures and that measuring errors at flight level may be strongly amplified, see Schwarz (1973).

Keeping these reservations in mind, table 7.1 can be interpreted. Mean gravity anomalies are given for different block sizes using various profile spacings and different assumptions on the measuring errors. The best combination of data has been determined in each case by the results summarized at the end of section 5. There are three important comclusions:

a.) The accuracies for all block sizes are in a range which will make them very useful for geodetic applications. With a profile spacing of 1° standard errors of $\pm$ 3 mgal for $5^\circ \times 5^\circ$ blocks and of $\pm$ 5 mgal for $1^\circ \times 1^\circ$ blocks can be achieved. With a profile spacing of $0^\circ.3$ standard errors of $\pm$ 3 mgal for 15' x 15' and 5' x 5' blocks are obtainable. It should be noted, however, that correlations will be larger for the 5' x 5' means especially if the standard errors of the Δg-values are large.

b.) The influence of measuring errors is more pronounced for small blocks than for large ones. This becomes even more apparent if always the same data combination is used which has not been done in table 7.1.

c.) The difference between the regional and the local covariance function shows clearly for large block sizes. Standard errors are about the same for blocks smaller than $1^\circ \times 1^\circ$. For larger blocks the results obtained by the regional function

Block Size	Profile Distance	Regional Covariance Function Standard Errors in mgal					Local Covariance Function Standard Errors in mgal				
	(m_g =)	± 1mgal	± 5mgal	± 1mgal	± 5mgal	± 20mgal	± 1mgal	± 5mgal	± 1mgal	± 5mgal	± 20mgal
	(m_{gg} =)	± 1E	± 1E	± 5E	± 5E	± 1E	± 1E	± 1E	± 5E	± 5E	± 1E
5°x5°	5°.0	± 8.5	± 8.6	± 9.1	± 9.2	± 10.0	± 2.6	± 2.7	± 2.7	± 2.8	± 3.3
	2°.5	± 4.2	± 4.5	± 5.4	± 5.6	± 7.2	± 2.1	± 2.3	± 2.3	± 2.5	± 3.0
	1°.0	± 3.2	± 3.5	± 3.5	± 3.8	± 5.9	± 1.6	± 1.8	± 1.8	± 2.0	± 2.7
1°x1°	1°.5	± 10.3	± 11.0	± 12.7	± 13.2	± 15.6	± 7.4	± 8.3	± 9.2	± 9.8	± 10.9
	1°.0	± 5.6	± 7.0	± 8.8	± 9.6	± 13.0	± 4.2	± 5.7	± 6.6	± 7.6	± 9.6
	0°.5	± 1.5	± 3.4	± 3.2	± 4.9	± 7.6	± 1.3	± 3.1	± 2.5	± 4.4	± 6.4
15'x15'	0°.5	± 3.1	± 4.8	± 5.2	± 6.4	± 8.2	± 2.4	± 3.8	± 4.2	± 5.3	± 6.9
	0°.3	± 1.7	± 2.5	± 3.0	± 5.7	± 5.2	± 1.5	± 2.3	± 2.4	± 5.1	± 3.6
	0°.2	± 1.2	± 1.8	± 2.1	± 3.6	± 5.0	± 1.1	± 1.5	± 1.8	± 3.1	± 3.8
5'x5'	0°.3	± 2.3	± 2.7	± 4.6	± 5.6	± 5.4	± 1.9	± 2.5	± 3.9	± 4.9	± 4.1
	0°.2	± 1.9	± 2.3	± 3.5	± 4.8	± 5.1	± 1.8	± 2.0	± 3.2	± 4.3	± 3.9
	0°.1	± 1.7	± 2.2	± 2.8	± 4.4	± 5.1	± 1.5	± 1.9	± 2.4	± 3.8	± 3.9

Table 7.1 : Accuracy of mean block values from a combination of gravity and gradiometer data.

are certainly more reliable. If we assume isostatic anomalies for the sea surface their covariances are probably well represented by the local covariance function.

8. Combination with Satellite Altimetry.

So far, we have estimated Δg-values from first and second order gravitational gradients only. When using measurements from satellite altimetry we are not just adding a new set of data but we are introducing a very different type of observations. They belong to a class of functions which is smoother than that of the estimated values. This can simply be seen from Stokes' integral where geoidal undulations are determined by integrating gravity anomalies. Reversing the process of integration will lead to a number of intricate mathematical problems. It is this problem we are dealing with and the difficulties connected to the so-called inversion of Stokes integral are hidden in our approach, too.

The smoothness of the altimeter data will produce a sort of basic standard error in the Δg-estimation. By this we mean that even with an ideal data distribution and errorless data we will not be able to push the standard error of estimation below a certain limit. Furthermore, numerical instabilities will occur if the point density exceeds a certain measure. From practical considerations it is important to find the optimal point distance where the basic standard error can be obtained with a minimum number of points and profiles. Also, the critical distance where instabilities are likely to occur should be known in order to provide safeguards in the program.

The same configuration as in section 4 and 5 has been used to estimate gravity anomalies from geoidal undulations and to determine the two characteristic distances. The standard error of the altimeter data has been varied between 0 m and $\pm$ 5 m.

Only the regional covariance function has been used in this case. Results are shown in fig. 8.1 where the error of estimation is given as a function of the profile distance for different accuracies of the altimeter data. The numbers written to the curves are standard errors in meter units. Let us first consider pure interpolation, i.e. the curve numbered 0. The standard error levels off at a profile distance of about $0^{\circ}.2$ and becomes erratic at about $0^{\circ}.08$. Profile distances smaller than this critical value will give completely irregular results including imaginary standard errors. The critical value is dependent on the internal accuracy of the computer and there is also some dependence on the point configuration. Thus, for double precision arithmetic a critical distance of $0^{\circ}.1$ is necessary to secure a stable solution. On the other hand, the optimal distance is at about $0^{\circ}.2$ and measurements with a denser profile spacing will not improve the solution. For mean values the critical distance stays the same, while the optimal distance increases with growing blocks size. Thus, we have optimal distances of about $0^{\circ}.4$ and $0^{\circ}.8$ for $1^{\circ} \times 1^{\circ}$ and $5^{\circ} \times 5^{\circ}$ blocks. Using these values we are able to determine the basic standard error which is $\pm$ 19.5 mgal for point values, $\pm$ 6.5 mgal for $1^{\circ} \times 1^{\circ}$ blocks, and $\pm$ 3.0 mgal for $5^{\circ} \times 5^{\circ}$ blocks. For blocks smaller than $1^{\circ} \times 1^{\circ}$, correlations become so large that it is misleading to give standard errors as estimates of accuracy.

If we turn from pure interpolation to interpolation including measuring errors we can observe some interesting features from fig. 8.1. Growing standard errors of the altimeter data will result in a larger optimal distance and in a flattening of the error curves. At $m_N = \pm 1m$ we have an almost linear slope for the error of estimation. Judging from the set of curves the optimal distance is at about 1° in that case and the apparent increase in accuracy with smaller profile distances must be regarded as fictitious. Furthermore, we have stable solutions even for very small profile distances. Thus, the incorporation

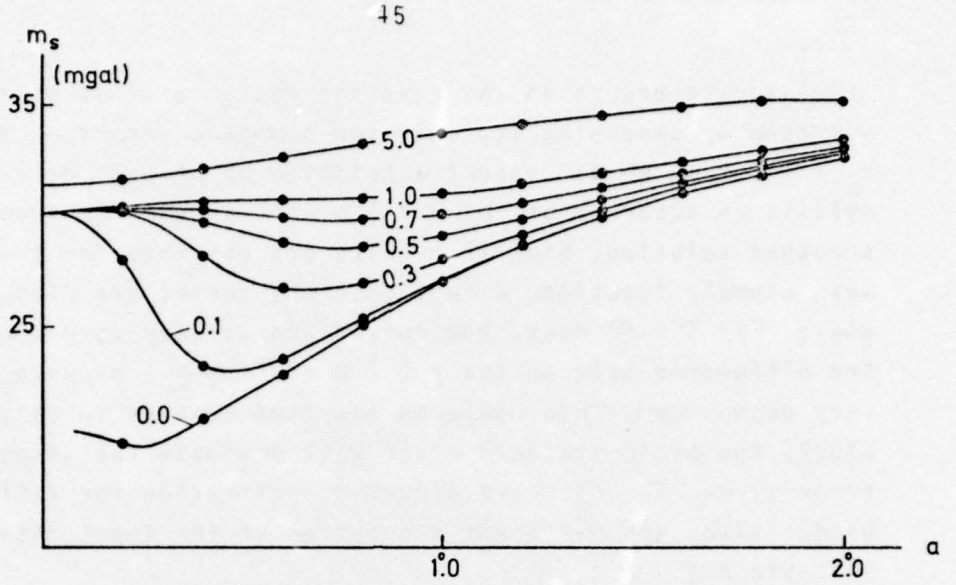

Fig.8.1 Estimation of Δg-values from altimeter data only.

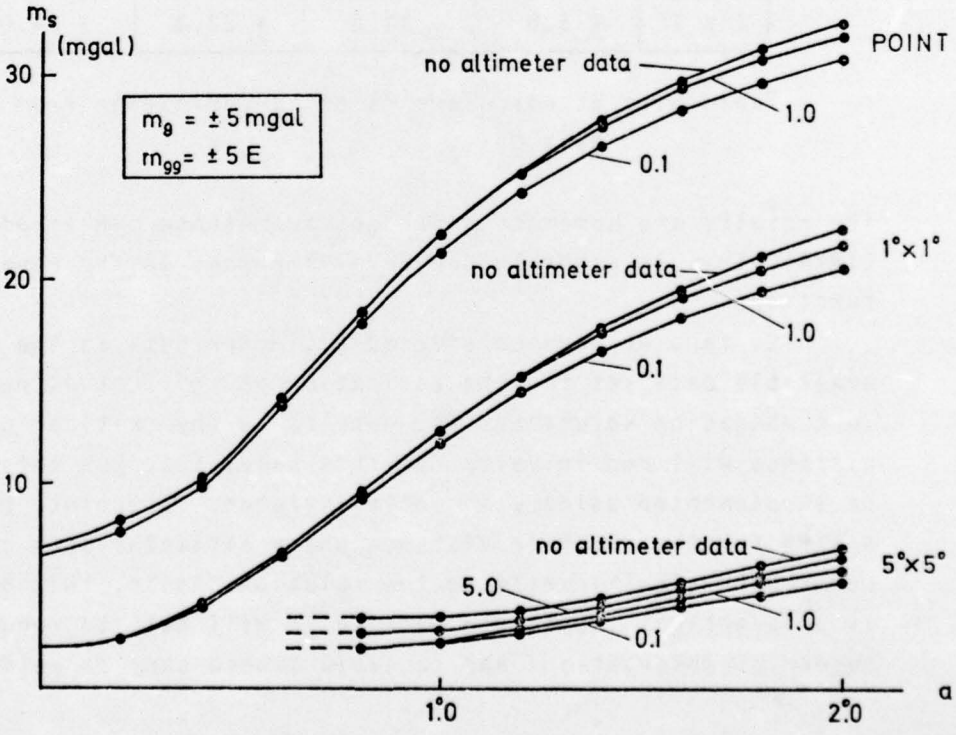

Fig.8.2 Combination of gradiometer and altimeter data.

of measuring errors in the equation system will stabilize the solution by smoothing it. Only for standard errors of about $m_N = \pm 0.1$ m we can expect a solution which will recover some detail, an accuracy of $m_N = \pm 1$ m will already produce a strongly smoothed solution. Similar results are obtained for the $1^\circ \times 1^\circ$ mean anomaly function, except that the curves are flatter on the whole. For $5^\circ \times 5^\circ$ means the curves are already very smooth and the difference between the ± 0.1 m and the ± 1 m curve is not very pronounced. This could be expected because in case of large blocks the basic standard error will dominate the shape of the error curve. The standard errors of estimation for different blocks sizes and different accuracies of the input data are given in table 8.1:

Block size	Standard error of estimation in mgal for m_N =			
	$\pm$ 0.1 m	$\pm$ 1.0 m	$\pm$ 5.0 m	$\pm$ 10.0 m
$5^\circ \times 5^\circ$	$\pm$ 3.0	$\pm$ 4.1	$\pm$ 6.5	$\pm$ 7.9
$1^\circ \times 1^\circ$	$\pm$ 6.8	$\pm$ 14.6	$\pm$ 22.3	$\pm$ 24.0

Table 8.1: Standard errors of Δg-estimation from altimeter data only.

The results are somewhat different from those published by Rapp (1974). This is probably due to differences in the covariance functions.

So far, we have considered altimeter data as the only available data set for the estimation of Δg . Let us now turn to combination solutions. The results on the critical and optimal distance will remain valid for this case, too. But they have to be supplemented using a somewhat different viewpoint. We are now asking for that profile distance where altimeter data cease to contribute significantly to the solution. Again, this question is of practical importance because it will help to reduce the number of observations and to avoid unnecessary correlations.

Fig. 8.2 shows the error of estimation as a function of the profile distance for combination solutions with and without altimeter data and for blocks of different sizes. The standard errors of the altimeter measurements have been varied while standard errors of the other quantities have been held fixed. Point estimation has been included as a limiting case and because it permits a direct comparison with previous results. Since the simple configuration as in fig. 8.1 has been used this is not true for the mean values. Their standard errors will need a scaling. The standard errors of the altimeter data have again been written to the curves. There are three obvious results. First, the accuracy of the $5^\circ \times 5^\circ$ mean values will always be improved when using satellite altimetry. Second, for blocks of $1^\circ \times 1^\circ$ and smaller, satellite altimetry will not contribute significantly if the profile spacing is smaller than 1° . It is also at this distance that the standard error of the $5^\circ \times 5^\circ$ blocks levels off indicating that a denser spacing will not improve the accuracy. Third, an improvement in the altimeter accuracy from $m_N = \pm 1.0$ m to $m_N = \pm 0.1$ m will improve the accuracy of the combination solution by only about 5 % . These results have been checked and confirmed by computing a number of cases in table 7.1 from a combination of gravity, gradiometer, and altimeter data. Finally, it should be remembered that the standard errors of Δg and of the second-order gradients have been chosen rather large. If they are smaller, the contribution of satellite altimetry to blocks of $1^\circ \times 1^\circ$ and smaller sizes will be even less significant.

9. Numerical Problems.

In this section we will first treat the question of numerical stability in a more comprehensive way and then discuss some simplifications in the inversion of the covariance matrix C_{xx} . Again, questions of practical solvability will be more important than mathematical rigour.

Instabilities may occur in two cases. First in the downward continuation from flight level to sea level and second in the estimation of Δg from altimeter data only. In the first case the smoothness of the data function is due to attenuation and dependent on the size of s in equation (3.12). In the second case the data function has a lower order of smoothness than the function to be estimated. This is apparent from the coefficients k_n in the covariance models. From a practical point of view both problems can be treated in a similar way because the quantity

$$t_n = s^{n+1} k_n \qquad 9.1$$

represents a damping of the original coefficients in both models and therefore high frequencies cannot properly be recovered.

If we have an unstable linear system

$$x = As \qquad 9.2$$

we can regularize the solution by augmenting the diagonal of the system of normal equations by small amounts, i.e. by adding a matrix αI . We obtain

$$s = (A^T A + \alpha I)^{-1} A^T x \qquad 9.3$$

as a solution and the usual minimum condition of least-squares adjustment is replaced by

$$\| As - x \|^2 + \alpha \cdot \| s \|^2 \rightarrow \text{minimum} \qquad 9.4$$

where $\| \cdot \|^2$ denotes the square norm. This method of regularization is due to Tihonov (1965) and it is valid even in cases when the operator A is nonlinear. As can be seen from the

condition (9.4) strong variations of the solution are prevented by imposing a restriction on the norm of the solution. In practice, the determination of α is a difficult problem, see Ivanow (1966). If it is chosen too small, we will have residual instabilities. If it is made too large, the solution will be too smooth and the optimum will not be reached. Usually one has to rely on trial and error. An interesting numerical example is given in Tikhonov and Glasko (1964) where some of the computational difficulties are discussed.

It has been pointed out in Schwarz (1973) that in case of a linear system there is a close connection between Tihonov's method and least-squares collocation. A similar argument can be used in our case. The variances σ_i in equation (4.4) can be interpreted as regularizing factors. However, they are given in advance by the accuracy of the data and have not been determined by a best approximation of some kind. It is therefore still necessary to find an optimal coefficient α and to see by comparison how much we loose by being bound to the given σ_i. In other words, because we must use an actual variance our solution will usually be too smooth. Only if our data are given with a very high accuracy we can hope to approach the optimal α. To give more practical meaning to this concept let us return to fig. 8.1. The coefficients α can be obtained by squaring the standard errors and it is quite obvious that an optimal solution must have $\alpha<0.01$. The loss of information with growing α is considerable and apparently the difference between $\alpha=0.01$ and $\alpha=1.0$ is not only of a quantitative but also of a qualitative manner. More detailed results can be obtained from simulation studies where the exact functions are known and an independent control is possible.

A different approach to the problem is provided by looking at its spectral representation. Using formulas (3.12) and (9.1) we can write

$$K(P,Q) = A \sum_{n=0}^{\infty} t_n P_n(\cos\psi) \qquad 9.5$$

where the coefficients t_n are a smoothed version of the original k_n . The smoothing is dependent on the degree n . It is generated by a factor v^{n+1} in case of attenuation and by a factor $R^2/(n-1)^2$ in case of altimeter data. The quantity v is defined by

$$v = \frac{R^2}{(R+h)^2}$$

where h is the flying altitude. In our estimation procedure we are basically trying to recover the original coefficients k_n . Errors in the data will falsify the coefficients t_n by small amounts. Let us assume for a moment that we have a small error of equal size in each coeficient t_n . When we try to recover the quantities k_n , the effect of this error will be very different depending on the degree of the coefficient. For low degrees we will have an amplifying factor close to one and no difficulties will arise. For high degrees the amplifying factor may be arbitrarily large. Thus, our solution will become completely meaningless if we try to include all high frequencies. To overcome this difficulty some sort of filtering must take place. This filtering procedure is the analogue to the determination of an optimal α . In one case we are considering the frequency domain, in the other case the time domain. The filtering of the high frequencies will as before produce a smoothing of the solution. The extent of the smoothing will depend on the characteristics of the smoothing factors as well as on the accuracy level of the data. In our problem the smoothing of the high frequencies is much stronger in case of satellite altimetry. The accuracy level of the data can be related to the effects of the filtering process in the frequency domain. Eigenvalue techniques as in Schwarz (1975) could be used for this purpose. They will allow interesting comparisons with the results presented in fig. 8.1. Thus, it is important to take into account both aspects of the stability problem in order to give a meaningful interpretation to the numerical results.

Let us finally consider the inversion of the matrix C in equation (4.1). Since the inversion is the time-consuming part in the algorithm, it will strongly influence the efficiency of the program. Some general rules have already been given in section 4 how to reduce the number of measurements and by this the size of the matrix. We shall therefore concentrate on simplifications arising from the structure of the matrix. Table 9.1 shows the covariance matrix for the optimal data combination as given in section 5 including altimeter data. Only one measured point is considered.

	N	Δg	$T_{\lambda\lambda}$	$T_{\phi\phi}$	$T_{\phi r}$	$T_{\lambda r}$
N	+	+	+	+	(0)	0
Δg		+	+	+	(0)	0
$T_{\lambda\lambda}$			+	+	(0)	0
$T_{\phi\phi}$				+	(0)	0
$T_{\phi r}$					+	0
$T_{\lambda r}$						+

Table 9.1 Structure of the C_{xx}-matrix for one point

The variances and covariances of the upper half of the symmetrical matrix are shown. The notations are as follows:

0 ... covariance is zero for all ψ

(0)... covariance is zero for $\psi = 0$

\+ ... variance and covariance have a value.

The crosscovariances implying $T_{\lambda r}$ form a diagonal submatrix which can directly be inverted. In this way more than 20 % of the computing time for the inversion may be saved. Furthermore, there are some zero-bands connected with $T_{\phi r}$ and zeros from other crosscovariances may be matched with certain profile spacings. This will not influence the speed of inversion but will make the procedure more stable because a number of off-diagonal terms will become zero. It may also be possible to introduce in advance a

simple form of pivoting by considering the size and the shape of the different covariance functions and by ordering them accordingly. Thus, a careful assessment of the matrix structure may help to speed up and stabilize the inversion.

10. Conclusions

The preceding investigations have shown that a combination of first and second order gravitational gradients measured at flying altitudes will supply mean gravity anomalies at ground level accurate enough for geodetic applications. The results fall roughly into two groups. Those which are basically independent of the chosen covariance function and those which are not. Results of the first group may be summarized in six points:

1. The accuracy of an interpolated gravity anomaly is mainly dependent on its distance to the nearest profile. Therefore, a dense profile spacing is more important for interpolation than cross profiles. Cross profiles should be used for updating only.
2. A dense sequence of points along the profile is only necessary for integrating first-order gradients. For interpolation of Δg-values a density between 1/4 and 1/2 of the profile spacing will be sufficient.
3. For profiles with an arbitrary azimuth an optimal data combination should include:

   Δg, $T_{r\phi}$, $T_{r\lambda}$, $T_{\phi\phi}$, $T_{\lambda\lambda}$ for large profile spacings ($> 0^{\circ}3$)

   Δg, $T_{r\phi}$, $T_{r\lambda}$, T_{rr} for small profile spacings ($< 0^{\circ}3$).

   The inclusion of more second-order gradients will only slightly improve the accuracy. A smaller number of gradients may be used in special cases.

4. The influence of measuring errors is also different for large and for small profile spacings. In the first case the accuracy of the gradiometer values is most important while in the second case a high accuracy of gravity anomalies and second-order gradients is essential.
5. When estimating mean values the covariance function has to be changed in a similar way as for upward continuation. Thus, for a given block size the effects of downward continuation and of mean value determination will cancel at a certain altitude.
6. The combination of first and second order gradients with satellite altimetry will essentially contribute to the estimation of $5^\circ \times 5^\circ$ means. With present day accuracy only marginal improvements can be expected for $1^\circ \times 1^\circ$ blocks. For blocks of smaller size altimetry should not be used because correlations introduced by these data may impair the accuracy.

The following results are dependent on assumptions made about the covariance functions. These functions have been varied in a rather wide range so that it should be possible to estimate the effect of a change in one of the essential parameters. When actual gradiometer measurements become available, the basic assumptions can be checked and appropriate changes be made if necessary. Under these premises we can say:

7. Mean gravity anomalies can be estimated from first and second order gradients at a flight level of 10 km with the following accuracies. With a profile spacing of 1° standard errors of $\pm$ 3 mgal for $5^\circ \times 5^\circ$ blocks and of $\pm$ 5 mgal for $1^\circ \times 1^\circ$ blocks can be achieved. With a profile spacing of $0^\circ.3$ standard errors of $\pm$ 3 mgal are obtainable for blocks of 15'x 15' and 5'x 5'. It should be noted, however, that correlations may be large for the 5'x 5' blocks depending on the accuracy of the Δg-values. The influence of measuring errors is more pronounced for small blocks than for large ones. More details can be found in table 7.1 of this report.

The method used in this accuracy study is least-squares collocation. Its great flexibility has been demonstrated in

handling problems as different as the combination of heterogeneous data, interpolation, downward continuation and mean value estimation. Its numerical advantages have been shown in discussing the stability problem which is essential in the treatment of the above applications.

ACKNOWLEDGEMENTS

The writer wishes to thank Prof.Dr. H. Moritz for his encouragement and his patience in discussing many details of this report. Dr. R. Rummel has given valuable comments in an early stage of the work. C.C. Tscherning provided the COVAX-Subroutine in advance of publication and computations have been greatly facilitated by its use. Computer time has been made available by the Instruction and Research Computer Center of the Ohio State University and by the Rechenzentrum Graz, Austria.

REFERENCES

R. Bellman (1970): Introduction to Matrix Analysis. New York.

K.R. Britting (1971): Inertial Navigation Systems Analysis. New York.

Ch. Broxmeyer (1964): Inertial Navigation Systems. New York.

E. Grafarend (1972): Three Dimensional Geodesy and Gravity Gradients. OSU Report No 174.

E.J. Hannan (1970): Multiple Time Series. New York.

R.A. Hirvonen (1962): On the Statistical Analysis of Gravity Anomalies. Publications of the Isostatic Institute of the IAG, No 37, Helsinki.

V.K. Ivanow (1966): The Approximate Solution of Operator Equations of the First Kind. Zh. vychisl. mat. i. Mat.; Fiz. 6,6.

W.M. Kaula (1966): Statistical and Harmonic Analysis of Gravity. Army Map Service, Technical Report No 24, Washington.

T. Krarup (1969): A Contribution to the Mathematical Foundation of Physical Geodesy. Publications of the Danish Geodetic Institute, No 44, Copenhagen.

G. Lachapelle (1975): Determination of the Geoid Using Heterogenous Data. Mitteilungen der geodätischen Institute der TH Graz, Folge 19.

J.G. Marsh and S. Vincent (1974): Global Detailed Geoid Computation and Model Analysis. GSFC-Report x-921-74-131, Greenbelt.

P. Meissl (1970): Probabilistic Error Analysis of Airborne Gravimetry. OSU Report No 138.

P. Meissl (1971): A Study of Covariance Functions Related to the Earth's Disturbing Potential. OSU Report No 151.

E.H. Metzger and A. Jircitano (1974): Analysis of real time mapping of horizontal and vertical gravity anomalies aboard a moving vehicle such as an aircraft. Proceedings, International Symposium on Applications of Marine Geodesy, Columbus, Ohio, published by Marine Technological Society, Washington, D.C..

H. Moritz (1967): Kinematical Geodesy. OSU Report No 92.

H. Moritz (1971): Kinematical Geodesy II. OSU Report No 165.

H. Moritz (1974): Some First Accuracy Estimates for Applications of Aerial Gradiometry. OSU Report No 209.

H. Moritz (1975): Combination of Aerial Gravimetry and Gradiometry. OSU Report No 223.

H. Moritz (1976): Covariance Functions in Least-Squares Collocation. OSU Report No 240.

R.H. Rapp (1974): Gravity Anomaly Recovery from Satellite Altimetry Data Using Least-Squares Collocation Techniques. OSU Report No 220.

R. Rummel (1975): Downward Continuation of Gravity Information from Satellite to Satellite Tracking or Satellite Gradiometry in Local Areas. OSU Report No 221.

K.P. Schwarz (1973): Investigations on the Downward Continuation of Aerial Gravity Data. OSU Report No 204.

K.P. Schwarz (1974): Tesseral Harmonic Coefficients and Station Coordinates from Satellite Observations by Collocation. OSU Report No 217.

K.P. Schwarz (1975): Zonale Kugelfunktionskoeffizienten aus Satellitendaten durch Kollokation. Deutsche Geodätische Kommission, Reihe C, Heft Nr. 209, München.

B. Szabo and D. Anthony (1971): Results of AFCRL'S Experimental Aerial Gravity Measurements. Bulletin Gëodësique, No 100.

A.N. Tihonov (1965): Incorrect Problems of Linear Algebra and a Stable Method for their Solution. Dokl. Akad. Nauk. SSSR, 163.

A.N. Tihonov and V.B. Glasko (1964): The Approximate Solution of Fredholm Integral Equations of the First Kind. Zh. vychisl. mat. i. Mat. Fiz. 4, 3.

C.C. Tscherning and R.H. Rapp (1974): Closed Covariance Expressions for Gravity Anomalies, Geoid Undulations, and Deflections of the Vertical Implied by Anomaly Degree Variance Models. OSU Report No 208.

C.C. Tscherning (1976): Covariance Expressions for Second and Lower Order Derivatives of the Anomalous Potential. OSU Report No 225.

List of Abbreviations

Dokl. Akad. Nauk	Doklady Akademii Nauk engl. edition: Soviet Mathematics-Doklady.
OSU Report	Reports of the Department of Geodetic Science, The Ohio State University, Columbus, Ohio.
Zh. vychisl. mat. i. Mat. Fiz.	Zurnal Vycislitel' noy matematiki i matematiceskoj Fiziki. engl. edition: USSR Computational Mathematics and Mathematical Physics.